2001-06

Vertical plane response of surface ships in close proximity towing.

Nash, Christopher A.

http://hdl.handle.net/10945/10993

NAVAL POSTGRADUATE SCHOOL
Monterey, California

THESIS

VERTICAL PLANE RESPONSE OF SURFACE SHIPS IN CLOSE PROXIMITY TOWING

by

Christopher Nash

June 2001

Thesis Advisor: Fotis A. Papoulias

REPORT DOCUMENTATION PAGE				Form Approved OMB No. 0704-0188
Public reporting burden for this collection of information is estimated to average 1 hour per response, including the time for reviewing instruction, searching existing data sources, gathering and maintaining the data needed, and completing and reviewing the collection of information. Send comments regarding this burden estimate or any other aspect of this collection of information, including suggestions for reducing this burden, to Washington headquarters Services, Directorate for Information Operations and Reports, 1215 Jefferson Davis Highway, Suite 1204, Arlington, VA 22202-4302, and to the Office of Management and Budget, Paperwork Reduction Project (0704-0188) Washington DC 20503.				
1. AGENCY USE ONLY *(Leave blank)*	**2. REPORT DATE** June 2001	**3. REPORT TYPE AND DATES COVERED** Master's Thesis		
4. TITLE AND SUBTITLE Vertical Plane Response of Surface Ships in Close Proximity Towing				**5. FUNDING NUMBERS**
6. AUTHOR(S) Christopher Nash				
7. PERFORMING ORGANIZATION NAME(S) AND ADDRESS(ES) Naval Postgraduate School Monterey, CA 93943-5000				**8. PERFORMING ORGANIZATION REPORT NUMBER**
9. SPONSORING / MONITORING AGENCY NAME(S) AND ADDRESS(ES) N/A				**10. SPONSORING / MONITORING AGENCY REPORT NUMBER**
11. SUPPLEMENTARY NOTES The views expressed in this thesis are those of the author and do not reflect the official policy or position of the Department of Defense or the U.S. Government.				
12a. DISTRIBUTION / AVAILABILITY STATEMENT Approved for Public Release; Distribution is Unlimited.				**12b. DISTRIBUTION CODE**

13. ABSTRACT ***(maximum 200 words)***

The purpose of this thesis is to analyze the vertical plane response of surface ships in close proximity towing. The problem is formulated by using the heave and pitch equations of motion in regular waves. The vertical motion of the leading and trailing ship attachment points is calculated. The relative motion between these points is then matched through a notional spring/damper model of the connection. This allows calculation of the complete response amplitude operators for the two ships in terms of their relative motion and connection force. Parametric studies are conducted in terms of connection spring and damper characteristics, speed, and sea direction. Regular wave results are extended in standard fully developed random seas. A notional example provides insight into future studies necessary to validate the close-proximity towing concept.

14. SUBJECT TERMS SLICE, KAIMALINO, SEAKEEPING, SWATH, RAO			**15. NUMBER OF PAGES** 102
			16. PRICE CODE
17. SECURITY CLASSIFICATION OF REPORT Unclassified	**18. SECURITY CLASSIFICATION OF THIS PAGE** Unclassified	**19. SECURITY CLASSIFICATION OF ABSTRACT** Unclassified	**20. LIMITATION OF ABSTRACT** UL

NSN 7540-01-280-5500

Standard Form 298 (Rev. 2-89)
Prescribed by ANSI Std. 239-18

THIS PAGE INTENTIONALLY LEFT BLANK

Approved for Public Release; Distribution is Unlimited

VERTICAL PLANE RESPONSE OF SURFACE SHIPS IN CLOSE PROXIMITY TOWING

Christopher A, Nash
Lieutenant, United States Navy
B.S., U. S. Naval Academy, 1994

Submitted in partial fulfillment of the
requirements for the degree of

MASTER OF SCIENCE IN MECHANICAL ENGINEERING

from the

NAVAL POSTGRADUATE SCHOOL
June 2001

Author: ______________________________
Christopher A, Nash

Approved by: ______________________________
Fotis A. Papoulias, Thesis Advisor

____
Terry R. McNelley, Chairman
Mechanical Engineering Department

THIS PAGE INTENTIONALLY LEFT BLANK

ABSTRACT

The purpose of this thesis is to analyze the vertical plane response of surface ships in close proximity towing. The problem is formulated by using the heave and pitch equations of motion in regular waves. The vertical motion of the leading and trailing ship attachment points is calculated. The relative motion between these points is then matched through a notional spring/damper model of the connection. This allows calculation of the complete response amplitude operators for the two ships in terms of their relative motion and connection force. Parametric studies are conducted in terms of connection spring and damper characteristics, speed, and sea direction. Regular wave results are extended in standard fully developed random seas. A notional example provides insight into future studies necessary to validate the close-proximity towing concept.

THIS PAGE INTENTIONALLY LEFT BLANK

TABLE OF CONTENTS

LIST OF FIGURES

LIST OF TABLES

THIS PAGE INTENTIONALLY LEFT BLANK

I. INTRODUCTION

A. PROBLEM STATEMENT

Towing of large payloads with small, power dense vessels is a proven means to cost effectively transport cargo. Divorcing the prime mover from the load bearing vessel results in a much larger payload fraction dedicated to cargo. This separation also allows the cargo vessel to be customized for special circumstances without altering the configuration of towing vessel. Another advantage is the reduced cost of utilizing a single sensor suite in the towing vessel to provide navigation and control of various cargo platforms. However, use of towing vessels has been limited to low speed, high payload barges. Several factors contribute to the traditional prejudices against using towing vessels for high-speed, medium payload operations. Conventional ocean going tow rigs employ long lines to diminish interaction forces between tug and tow. This results in poor maneuverability in constrained waterways. Large interaction forces result from the difference in response to a seaway between the tug and barge. Thus, high magnitude forces due to random seas result in peak amplitudes that render towing operations dangerous to personnel and equipment.

Until recently, the risks of high-speed towing have traditionally outweighed the rewards, leading to little interest in its development. Introduction of SWATH and related hull types such as SLICE that minimize sea surface interaction effects on vessels sparks renewed interest in the feasibility of high-speed towing based on the aforementioned advantages.

B. RESEARCH APPROACH

1. Table of Offsets Generation

With SLICE and KAIMALINO identified as suitable platforms for study, background data is generated for these vessels. SLICE lines drawings and the resultant table of offsets used as input into the modeling software were generated in "Seakeeping Characteristics of Slice Hulls..." by Lesh in six degrees of freedom. This study verifies the published displacements and operating characteristics of SLICE in six degrees of freedom. Existing hull lines and operating environment, i.e. salt water, regular wave response, and motion prediction in six degrees of freedom, are verified prior to development of KAIMALINO data files. Next, lines drawings of KAIMALINO are converted by hand to a table of offsets used in response prediction. KAIMALINO architecture is computed and verified against published characteristics provided by Lockheed-Martin Marietta Corporation. Table 1 summarizes this comparison and shows adequate agreement between published and calculated characteristics for parametric study of vessel response.

Vessel	Computed Displacement	Published Displacement	Length (LOA)	Beam	Draft
SLICE	165.5 LT	178 LT	105 FT	33/47 FT	14 FT
KAIMALINO	265 LT	217	88.25	40	15.25

Table 1. Modeled vs. Published Characteristics

2. Design Process

Basic fundamentals of naval architecture are employed to determine the feasibility of close-proximity towing operations. A commercial FORTRAN based code, SHIPMO is used to model motions of SLICE and KAIMALINO in a seaway. MATLAB based codes are used to verify individual ship motions, calculate vessel interactions, and predict regular and random wave response of the integrated towing unit. Graphics, parametric studies and product data are generated in the MATLAB environment.

THIS PAGE INTENTIONALLY LEFT BLANK

II. SHIP MOTION MODELING

A. OVERVIEW

Motion of a rigid body in 3-D space can be described in 6 degrees of freedom. Three translational (surge, sway, heave), and three rotational (roll, pitch, yaw) displacements are required. The diagram below illustrates these motions.

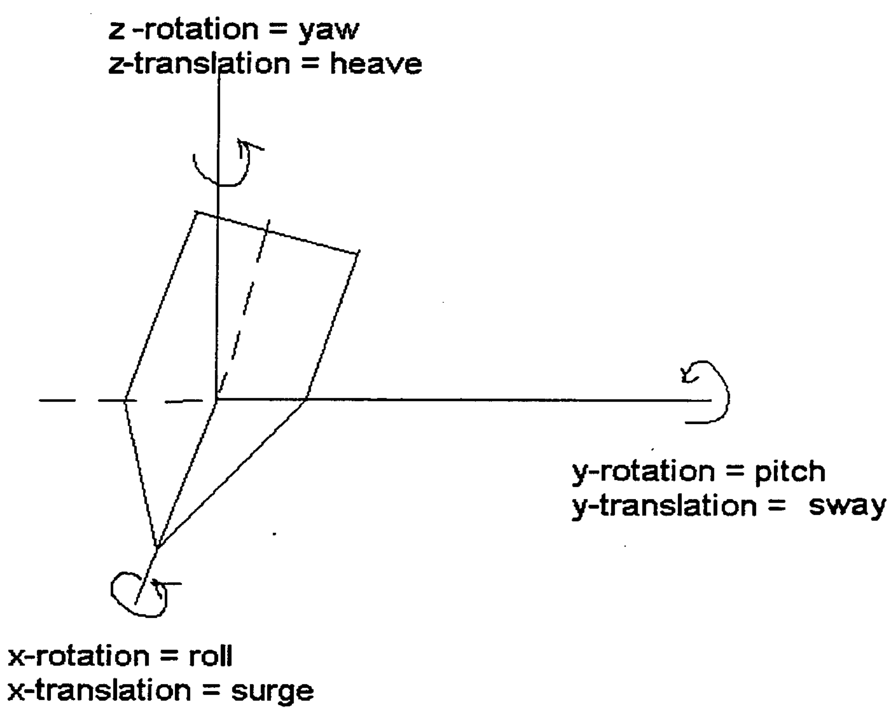

Figure 1. Rigid Body Model.

Rigid body motion includes velocity and acceleration components. Throughout this work and in the associated computer simulations, as well as in tables and figures, the following symbols will be used to describe ship's motion in a body reference frame.

Displacement	Velocity	Acceleration
$\eta_1 - surge$	$\dot{\eta}_1 - surge, vel$	$\ddot{\eta}_1 - surge, accel$
$\eta_2 - sway$	$\dot{\eta}_2 - sway, vel$	$\ddot{\eta}_2 - sway, accel$
$\eta_3 - heave$	$\dot{\eta}_3 - heave, vel$	$\ddot{\eta}_3 - heave, accel$
$\eta_4 - roll$	$\dot{\eta}_4 - roll, vel$	$\ddot{\eta}_4 - roll, accel$
$\eta_5 - pitch$	$\dot{\eta}_5 - pitch, vel$	$\ddot{\eta}_5 - pitch, accel$
$\eta_6 - yaw$	$\dot{\eta}_6 - yaw, vel$	$\ddot{\eta}_6 - yaw, accel$

Since both SLICE and KAIMALINO are modeled, a second subscript is added to each term to indicate the appropriate vessel. For SLICE, the second subscript is 's' and for KAIMALINO the subscript is 'k'. For example:

$$\eta_{1s} \rightarrow surge,\ SLICE$$
$$\dot{\eta}_{2k} \rightarrow sway\, velocity,\ KAIMALINO$$

B. MODELING A SHIP IN WAVES

1. Background

Ship response to head seas is "a complicated phenomena involving interactions between vessel dynamics and several distinct hydrodynamic forces" (Cummins). In other words, an arbitrary hull form will respond to a random sea state in a random, non-linear manner. However, a seaway's characteristics can be modeled and the ship's response approximated as linear. In a real seaway "six non-linear, differential equations of motion must be set up and solved simultaneously for six unknowns" (Cummins). Advanced calculus and hydrodynamics theories developed by Ogilivie, Cummins, and Wehausen have shown that response can be reduced into a Newtonian spring-mass-damper form that is frequency dependent. Further, in the case of slender hulls and moderate sea states the six non-linear equations reduce to two sets of three uncoupled equations. The longitudinal motions (surge, heave, pitch) are decoupled from the transverse motions (sway, roll, yaw).

2. Frequency Dependent Equations of Motion

A ship's interaction with a given seaway may be modeled as a spring-mass damper system, in its simplest form:

$$[M]\ddot{\vec{\eta}}+[B]\dot{\vec{\eta}}+[C]\vec{\eta}=[F_{ex}]$$

[M] = Mass of vessel and moments of inertia. (6x6)
[B] = Hydrostatic damping, due to energy dissipated in wave making. (6x6)
[C] = Restoring force and moment constants due to buoyancy. (6x6)
[F_{ex}] = Excitation forces and moments from seaway.

These equations provide a basis for understanding the model; the actual equations of motion are slightly more complex. First, the real [M] matrix includes inertia and cross coupling terms [m], and is summed with an "added mass" matrix [A]. An added mass coefficient corresponds to each of the degrees of freedom. The added mass terms represent additional mass and mass moments of inertia of seawater moved when a ship moves in any of the six degrees of freedom. Quite simply, it accounts for the mass that must be supplanted by the hull as it moves in any direction. The [F_{ex}] forces consist of the Froude-Kryloff and diffraction exciting forces and moments. The Froude-Kryloff force is due to the direct interaction between the body and the wave front. This interaction changes the hydrodynamic velocity profile from the undisturbed case, and creates the second element of the [F_{ex}] matrix, the diffraction force. The elements of the [A], [B],[C], [F_{ex}], and [m] matrices must be found to solve for the motions, η_k.

While the elements of the [C], [m], and [f_k] (Froude-Kryloff) can be found using analytic equations in "Principles of Naval Architecture, Vol III," the elements of the [A], [B], and [f_{diff}] (diffraction) matrices are found using "strip theory". Strip theory involves examination of a two-dimensional "strip" in the x-y plane of the vessel. "The flow field along this strip is approximated by the assumed two-dimensional flow along the strip" (Cummins). To obtain the effect on the entire vessel, all the strips are integrated along the ship's length. This process is repeated in each element to determine the second group of matrix elements above. For example: $A_{11} = \int_0^L a_{11} dx$. Further discussion of strip theory and the elements of the [A], [B], and [C] matrices are available in "Principles of Naval Architecture, Vol. III."

The other matrices and a more complete description of the equations of motion are:

$$[M]\ddot{\vec{\eta}} + [B]\dot{\vec{\eta}} + [C]\vec{\eta} = [F_{ex}]$$

[M] = [m+A] (6x6)

[B] = Hydrostatic damping, due to energy dissipated in wave making.

[C] = Restoring force and moment constants due to buoyancy.

[F_{ex}] = [$f_k + f_{diff}$] (6x1)

3. Equations of motion in the Frequency Domain

The equations of motion discussed above in the time domain are valid for zero forward motion in head seas. The matrix elements are valid for any given frequency of waves. To more accurately predict motions in waves for a given forward speed and wave angle, the frequency of encounter, ω_e dictates the values in the matrix elements. Since linear theory requires that vessel response be directly proportional to wave amplitude at the perceived frequency of incident waves, for regular waves, the vessel motions will be sinusoidal and have the form: $\vec{\eta}_k(t) = \bar{\vec{\eta}}_k e^{i\omega_e t}$, k=1...6 and $\vec{\eta}_k$ = complex amplitude of vessel response in the kth direction. The frequency of waves ω must therefore be shifted to account for vessel speed (V), and relative direction of encounter, (β). "Regular" or sinusoidal waves may be described by: $wave = \eta_o \cos(kx - \omega t)$

η_o -- wave amplitude

$\omega = 2\pi/T$

$k = 2\pi/\lambda$ -- wave number

In deep water where depth is greater than (λ/2), the dispersion relation states $\omega = \sqrt{kg}$. Thus for a given wavelength, wave frequency is known and the frequency of encounter is $\omega_e = (\omega - kV\cos(\beta))$.

Note that the time domain ODE's are linear, and the output motions are in complex form. It is evident then that the ODE's are easily transformed into the frequency domain, where the $\vec{\eta}_k$'s can be solved using algebraic methods.

$$
\begin{aligned}
\vec{\eta} &= \bar{\vec{\eta}} e^{i\omega_e t} \\
\dot{\vec{\eta}} &= i\omega_e \bar{\vec{\eta}} e^{i\omega_e t} \\
\ddot{\vec{\eta}} &= -\omega_e^2 \bar{\vec{\eta}} e^{i\omega_e t}
\end{aligned}
$$

Since the exponential exists in all terms, it is canceled and the equations of motion in the frequency domain become:

$$
\begin{aligned}
&-[m+A]\vec{\eta}\omega_e^2 + [B]i\omega_e\vec{\eta} + [C]\vec{\eta} = [\vec{F}_{ex}] \\
&if \rightarrow \bar{A} = -\omega_e^2[m+A] + [B]i\omega_e + [C] \\
&then \rightarrow \bar{A}\vec{\eta} = [\vec{F}_{ex}] \\
&and \rightarrow \vec{\eta} = inv(\bar{A})[\vec{F}_{ex}]
\end{aligned}
$$

C. SIMPLIFICATION OF EQUATIONS OF MOTION

1. Decoupling Transverse and Longitudinal Motion

The motions due to regular waves of a given wavelength and direction are now determined for a vessel with forward speed (V). Transverse and longitudinal motions are actually decoupled and may be solved as two distinct 3x3 systems vice the 6x6 system shown above. With this in mind, surge, heave and pitch responses and the resultant interactions between SLICE and KAIMALINO in these three degrees of freedom will be analyzed from this point forward. Surge motion may also be neglected because in long, slender ships, surge effects are small relative to heave and pitch. To simplify the equations of motion, all motions except η_3 and η_5 are set to zero. The expanded equations of motion in two degrees of freedom become:

$$\begin{bmatrix} \bar{A}_{33} & \bar{A}_{35} \\ \bar{A}_{53} & \bar{A}_{55} \end{bmatrix} \begin{bmatrix} \eta_3 \\ \eta_5 \end{bmatrix} = \begin{bmatrix} F_3 + f \\ F_5 + f x_s \end{bmatrix}$$

Analysis of the other degrees of freedom is possible with slight modifications of the matrix elements and variables of interest.

2. Data Generation and Computer Simulation

Elements of added mass, hydrostatic damping, and force matrices in the equations of motion are readily calculated using a motion analysis program that employs strip theory. The Fortran based code "Shipmo" is used to generate the data analyzed herein. "Shipmo" takes a table of offsets as input and calculates motions and added mass coefficients for a range of speeds and wave angles. The KAIMALINO table of offsets is hand generated from analysis of detailed scale drawings produced by Lockheed-Martin Marietta Corporation. The table of offsets is accepted along with a host of functional inputs such as wavelength, wave angle, forward speed, wave type, surge and roll damping, and the location of the position on the ship where the motion is to be analyzed.

Ship motions and the matrix coefficients are calculated for multiple speeds and wave angles, for wavelengths from twenty to one thousand feet. A database of "Shipmo" output files is created for both SLICE and KAIMALINO for speeds from zero to twenty knots in one-knot increments, and for wave angles from zero (following seas) to one hundred eighty degrees (head seas) in five-degree increments. The utilization of this database to predict the connection forces on a close-proximity tow is further discussed in the next section.

D. SLICE AND KAIMALINO MODELING AND INTERACTIONS

1. Ship Motion in Pitch, Heave at Connection Point

The integrated tow connection point on SLICE and KAIMALINO is chosen along the centerline, at deck height, at the aft-most point on SLICE and the forward-most point on KAIMALINO. Since heave and pitch are decoupled from sway and yaw, only the elements associated with heave and pitch and their cross coupling elements are needed to solve for η_3 and η_5.

$$\begin{array}{l} heave- \\ pitch- \end{array} \begin{bmatrix} \bar{A}_{33} & \bar{A}_{35} \\ \bar{A}_{53} & \bar{A}_{55} \end{bmatrix} \begin{bmatrix} \eta_3 \\ \eta_5 \end{bmatrix} = \begin{bmatrix} F_3 + f \\ F_5 + fx_s \end{bmatrix}$$

Using the A_{bar} factoring discussed above, the equations of motion for each vessel, with the bar removed for simplicity reduce to:

$$\begin{aligned}
A_{33,s}\eta_{3,s} + A_{35,s}\eta_{5,s} &= F_{3,s} + f_s \\
A_{53,s}\eta_{3,s} + A_{55,s}\eta_{5,s} &= F_{5,s} - f_s x_s \\
A_{33,k}\eta_{3,k} + A_{35,k}\eta_{5,k} &= F_{3,k} + f_k \\
A_{53,k}\eta_{3,k} + A_{55,k}\eta_{5,k} &= F_{5,k} - f_k x_k
\end{aligned}$$

f_k - connection force on KAIMALINO

f_s - connection force on SLICE

x_{sub} - distance from CG to connection point

Since f is a reaction force, $f = f_s = -f_k$.

The η's above cannot be solved directly. However, making the following substitutions the motion due to the excitation force ($\mu_{n,j}$) and the motion due to the connection force ($\nu_{n,j}$) may be solved individually assuming a unit connection force.

$$\begin{aligned}
\eta_{3,s} &= \mu_{3,s} + \nu_{3,s} f \\
\eta_{5,s} &= \mu_{5,s} + \nu_{5,s} f \\
\eta_{3,k} &= \mu_{3,k} + \nu_{3,k} f \\
\eta_{5,k} &= \mu_{5,k} + \nu_{5,k} f
\end{aligned}$$

Cramer's rule is used to solve for $\mu_{n,j}$ and $\nu_{n,j}$ in the following equations:

$$A_{33,s}\mu_{3,s} + A_{35,s}\mu_{5,s} = F_{3,s}$$
$$A_{53,s}\mu_{3,s} + A_{55,s}\mu_{5,s} = F_{5,s}$$
$$A_{33,k}\mu_{3,k} + A_{35,k}\mu_{5,k} = F_{3,k}$$
$$A_{53,k}\mu_{3,k} + A_{55,k}\mu_{5,k} = F_{5,k}$$

$$A_{33,s}\nu_{3,s} + A_{35,s}\nu_{5,s} = 1$$
$$A_{53,s}\nu_{3,s} + A_{55,s}\nu_{5,s} = -x_s$$
$$A_{33,k}\nu_{3,k} + A_{35,k}\nu_{5,k} = 1$$
$$A_{53,k}\nu_{3,k} + A_{55,k}\nu_{5,k} = -x_k$$

$$\mu_{3,j} = \frac{\begin{vmatrix} F_{3j} & A_{35,j} \\ F_{5j} & A_{55,j} \end{vmatrix}}{\begin{vmatrix} A_{33,j} & A_{35,j} \\ A_{53,j} & A_{55,j} \end{vmatrix}} \qquad \nu_{3,j} = \frac{\begin{vmatrix} 1 & A_{35,j} \\ -x_j & A_{55,j} \end{vmatrix}}{\begin{vmatrix} A_{33,j} & A_{35,j} \\ A_{53,j} & A_{55,j} \end{vmatrix}}$$

$$\mu_{5,j} = \frac{\begin{vmatrix} A_{33,j} & F_{3j} \\ A_{53,j} & F_{5j} \end{vmatrix}}{\begin{vmatrix} A_{33,j} & A_{35,j} \\ A_{53,j} & A_{55,j} \end{vmatrix}} \qquad \nu_{5,j} = \frac{\begin{vmatrix} A_{33,j} & 1 \\ A_{53,j} & -x_j \end{vmatrix}}{\begin{vmatrix} A_{33,j} & A_{35,j} \\ A_{53,j} & A_{55,j} \end{vmatrix}}$$

With $\mu_{n,j}$ and $\nu_{n,j}$ thus solved, the heave (η_3) and the pitch (η_5) may now be determined for an arbitrary connection force.

E. MODELING THE CONNECTION FORCE, F

1. Absolute Motion at the Connection Point

Having solved for the motions due to excitation forces ($\mu_{n,j}$) and the heave and pitch due to a unit connection force ($\nu_{n,j}$), superposition is now employed to find the overall heave and pitch of the two ships with a motion dependent connection force. Since rotational motion (pitch) will be unrestrained at the connection points, the connection force will be due to the difference in absolute translation of the two vessels at the connection point. The absolute motions at the connection points are described by:

$$\xi_s = \eta_{3,s} - \eta_{5,s} x_s \rightarrow \textit{Slice motion}$$
$$\xi_k = \eta_{3,k} - \eta_{5,k} x_k \rightarrow \textit{Kaimalino motion}$$

Notice the equations above cannot be solved until a connection force is supplied. However, because connection force is dependent on the difference in absolute motion of the two vessels, a theoretical relationship between the connection force and difference in absolute motion must be assumed. A generic spring-damper interface is inserted and the matching condition becomes:

$$f = k(\xi_s - \xi_k) + c(\dot{\xi}_s - \dot{\xi}_k) \rightarrow \textit{time domain}$$
$$f = (k + ic)(\xi_s - \xi_k) \rightarrow \textit{frequency domain}$$

Recall that the absolute motions are functions of the heave and pitch amplitudes:

$$\eta_{3,s} = \mu_{3,s} + \nu_{3,s} f$$
$$\eta_{5,s} = \mu_{5,s} + \nu_{5,s} f$$
$$\eta_{3,k} = \mu_{3,k} + \nu_{3,k} f$$
$$\eta_{5,k} = \mu_{5,k} + \nu_{5,k} f$$

The following sequence describes the mathematical steps of simplifying the matching condition using the heave and pitch amplitudes and simplifying variables:

$$\begin{aligned}
&\textit{if}: \\
&(\xi_s - \xi_k) = a - bf \rightarrow \textit{factored heave} - \textit{pitch amplitudes} \\
&\textit{and} \\
&(\xi_s - \xi_k) = \eta_{3s} - \eta_{3k} - x_s \eta_{5s} + x_k \eta_{5k} \\
&\textit{then} \\
&a = \mu_{3s} - \mu_{3k} - x_s \mu_{5s} + x_k \mu_{5k} \\
&b = \nu_{3s} - \nu_{3k} - x_s \nu_{5s} + x_k \nu_{5k} \\
&\textit{next let} \rightarrow K = (k + ic), \\
&\textit{so} \rightarrow f = K(a - bf) \\
&\textit{connection force} \rightarrow f = \frac{Ka}{1 + Kb}
\end{aligned}$$

The connection force is thus solved. Furthermore, the individual motions of each vessel and the corresponding connection force are dependent on vessel speed, seaway characteristics, and the spring-damper constants [$\eta_{n,j} = fun(\lambda, \beta, V, k, c)$].

2. Computer Modeling

Modeling of SLICE and KAIMALINO's response to regular waves is accomplished in all six degrees of freedom for a given set of input conditions as previously described. The purpose of this work is to further research the individual ship responses and develop a model that accurately predicts and if possible optimizes the connection force on a "hitch" connecting SLICE and KAIMALINO.

Vessel response and matrix coefficients of the motion variables are found in "Shipmo", which produces output files containing response and matrix data for reading in the MATLAB environment. These files are downloaded into the program "Samplemain" developed by Papoulias and improved by Nash to accommodate vertical and horizontal motions as inputs. "Samplemain" repeats some of the functions of "Shipmo", calculating heave and pitch response to a seaway as described in the preceding analytic discussions. The response is compared to the output of "Shipmo" prior to proceeding with matching condition and force calculations.

With the SLICE and KAIMALINO heave and pitch response verified, matching condition and connection force calculations are added to determine both the connection force for optimization purposes, and the front and rear ship heave and pitch response with a rigid connection attaching the two. The program is currently capable of determining the coupled heave/pitch response and connection force for user supplied spring-damper constants. With the existing strip theory database produced from "Shipmo" runs, this is possible for ranges of speed from (0-20) knots-every knot, wave angles (0-180) degrees-every five degrees, and is good for wavelengths from 20 feet to 1000 feet.

F. REGULAR WAVE RESULTS

Formulation of the equations of absolute motion at the connection point (ξ_s and ξ_k) and computer modeling discussed previously form the pillar for this research. The most interesting problem facing designers of a close-proximity towing system is engineering the connecting apparatus. The design must exhibit adequate strength to withstand the forces imposed by the differential motion of the two vessels. Using the mathematical model discussed above, and the MATLAB code "Samplemain.m", the absolute motion at the connection point and the resulting connection force is evaluated. The force is normalized for a one-foot wave height, and plotted with absolute motion versus wave frequency. Typical regular wave results are plotted for fifteen-knot forward speed and 180° wave angle (head seas). Absolute motion magnitude ($xi_s = |\xi_s|$, $xi_k = |\xi_k|$) and phase angle, and the connection force are plotted for different combinations of spring constant and damping coefficient values. With c=0, a small, medium, and large spring constant relative to displacement is chosen for comparison. A similar combination in damping coefficient is compared for k=0.

1. K=0 lbf/ft; C=0 lbf-s/ft

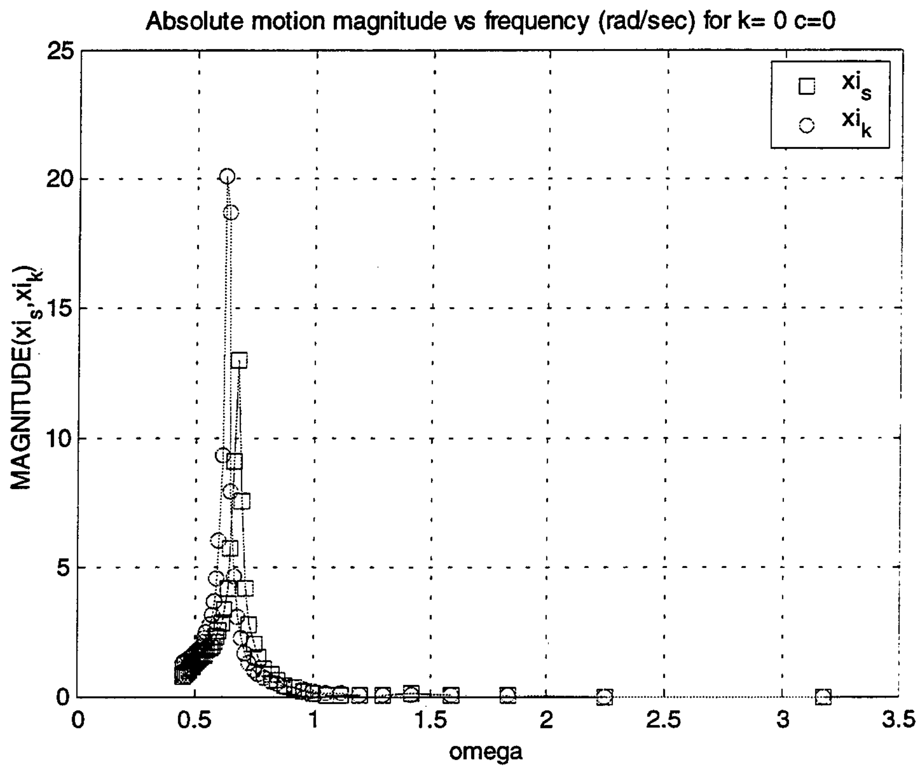

Figure 2. Absolute motion mag. K=0, C=0

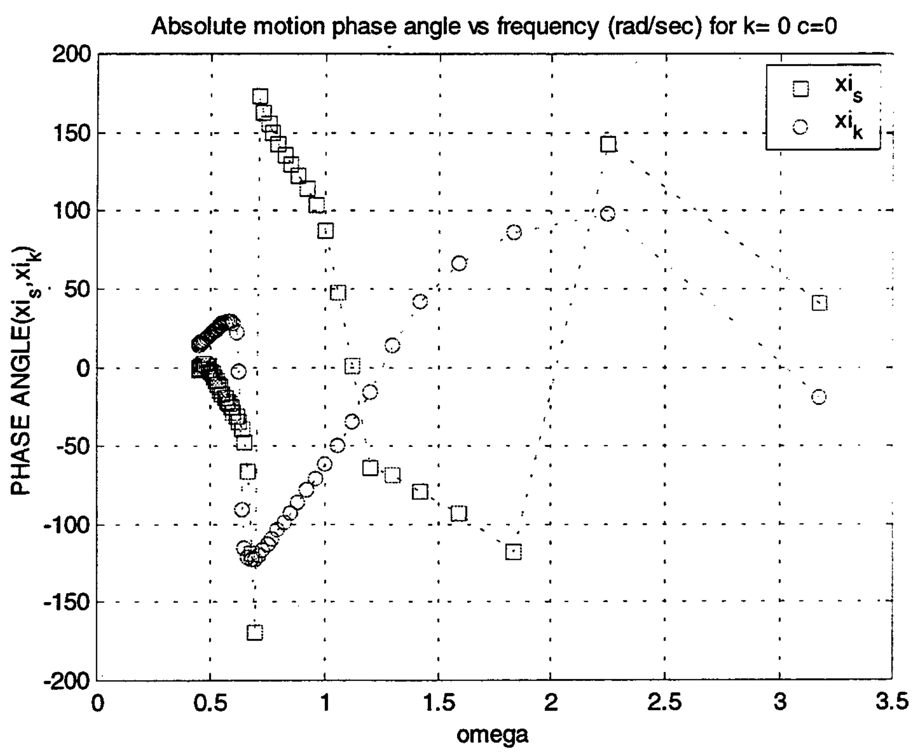

Figure 3. Absolute motion phase K=0, C=0

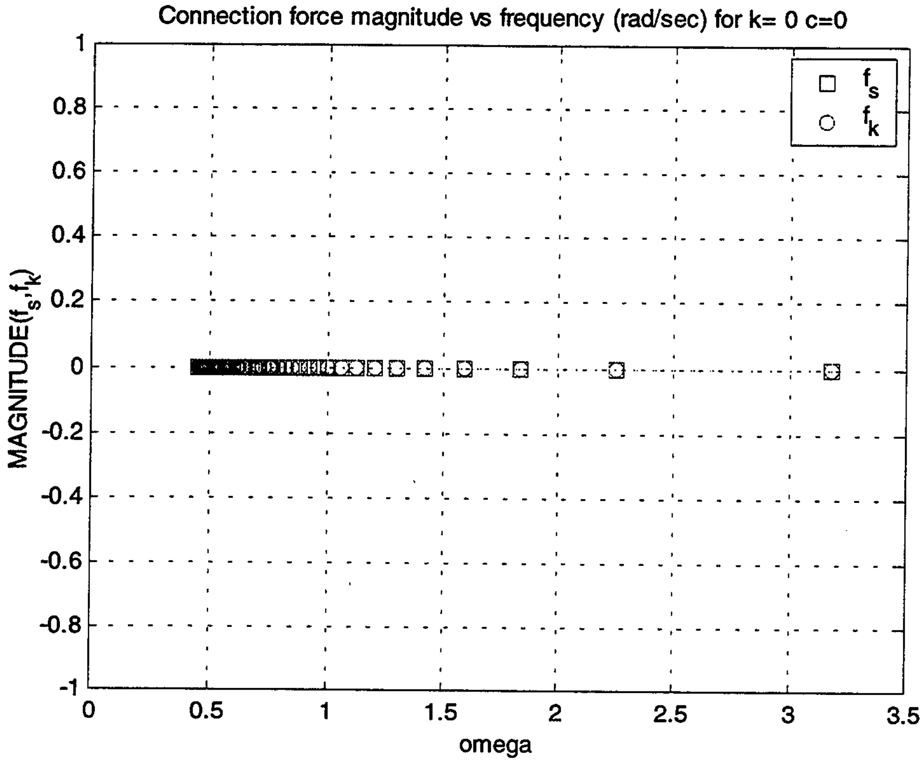

Figure 4. Force magnitude, K=0, C=0

2. K=5000 lbf/ft; C=0 lbf-s/ft

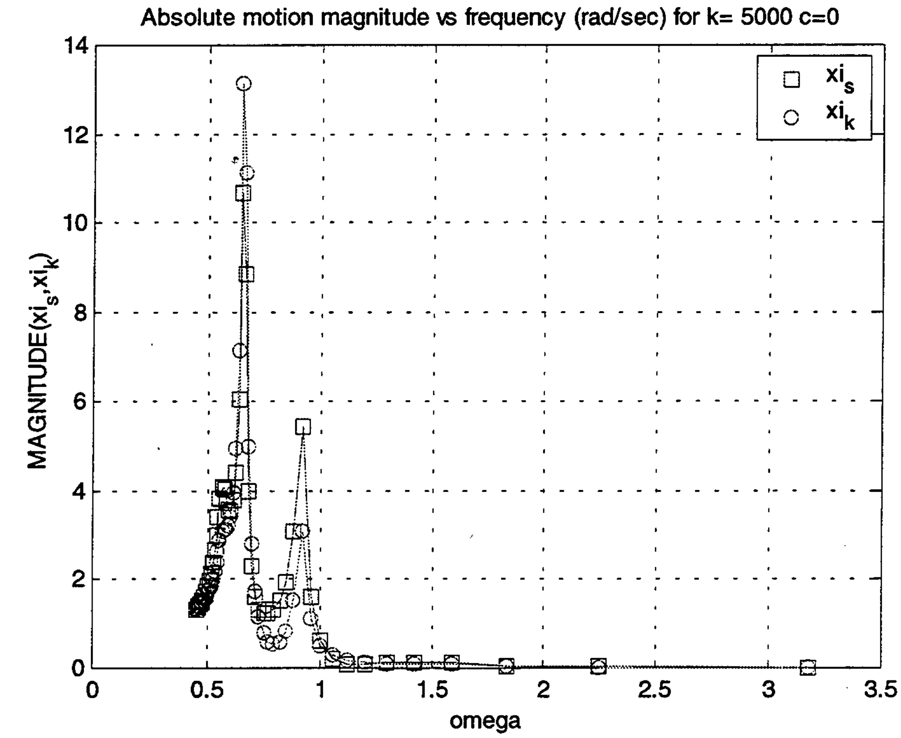

Figure 5. Absolute motion mag. K=5000, C=0

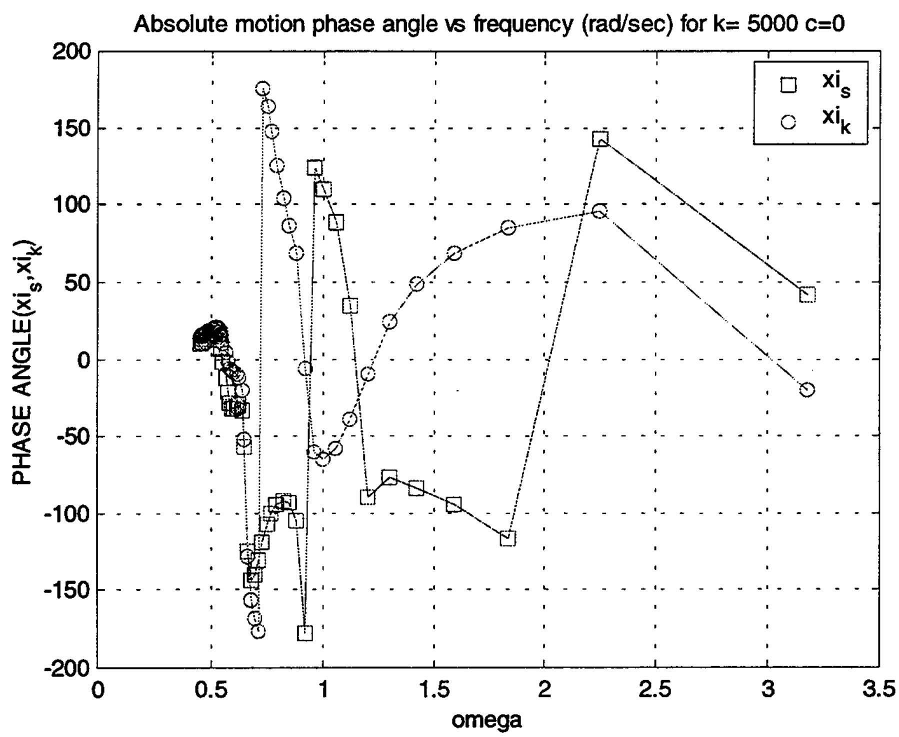

Figure 6. Absolute motion phase K=5000, C=0

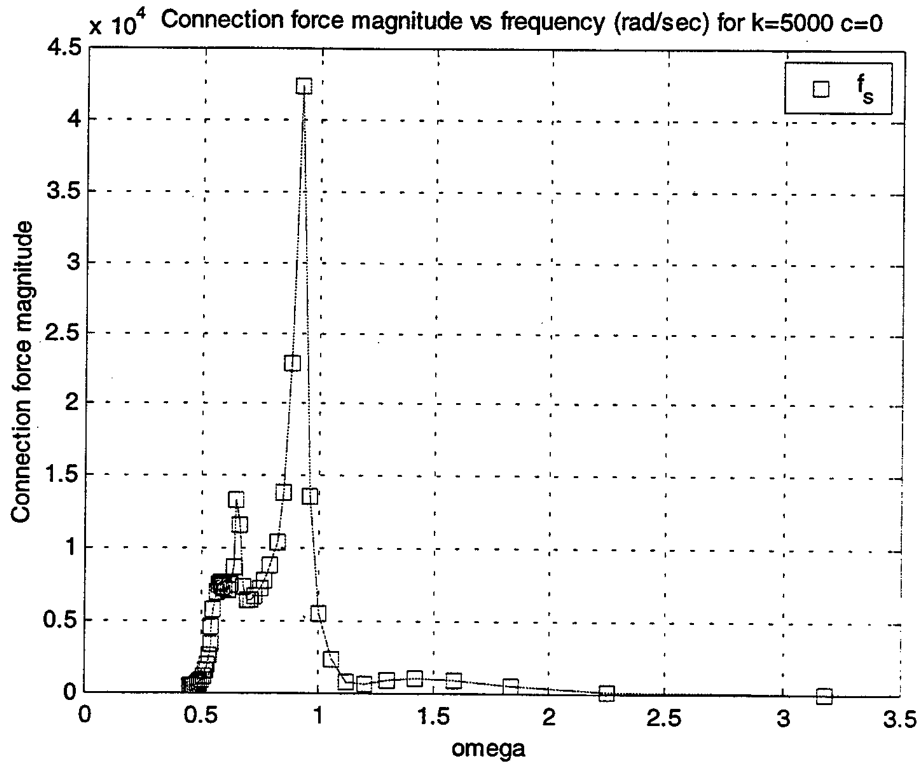

Figure 7. Force magnitude, K=5000, C=0

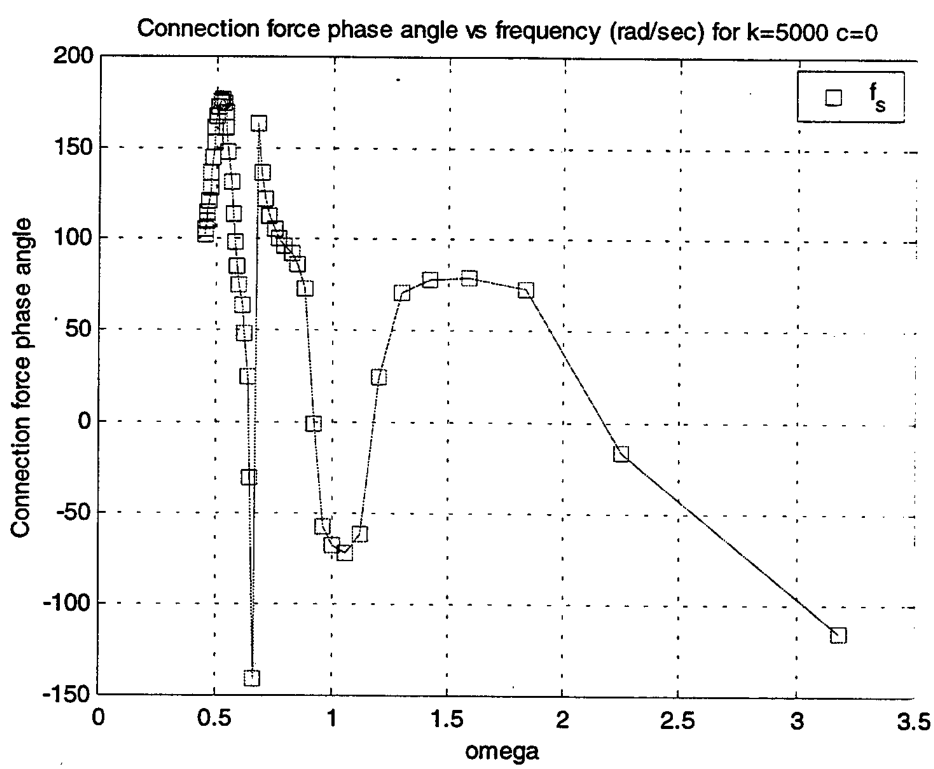

Figure 8. Force phase angle, K=5000, C=0

3. K=500000 lbf/ft; C=0 lbf-s/ft

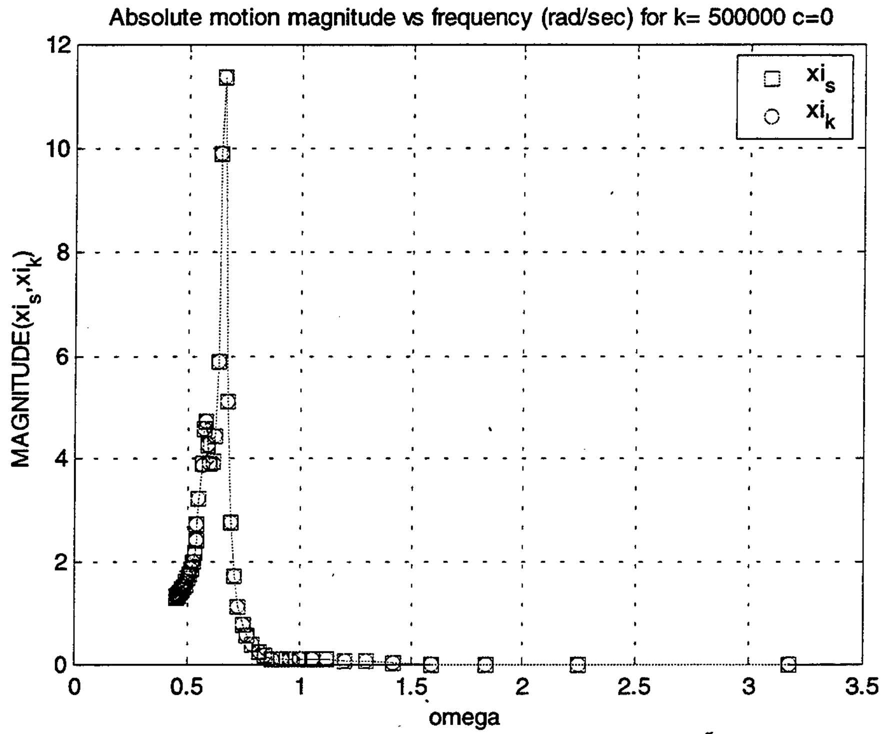

Figure 9. Absolute motion mag. K=5x10^5, C=0

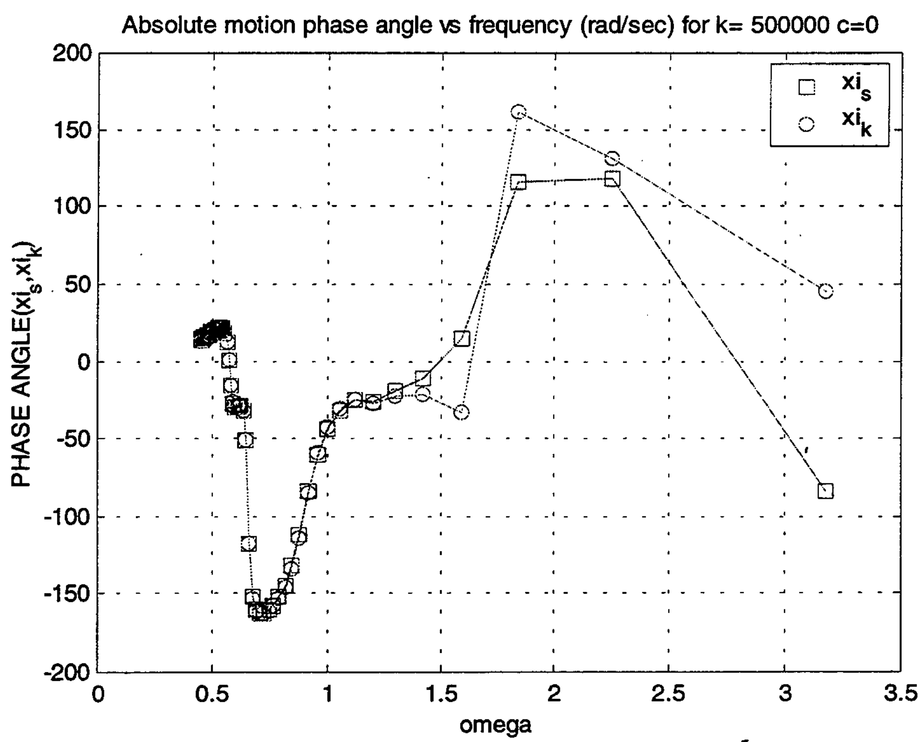

Figure 10. Absolute motion phase K=5x10^5, C=0

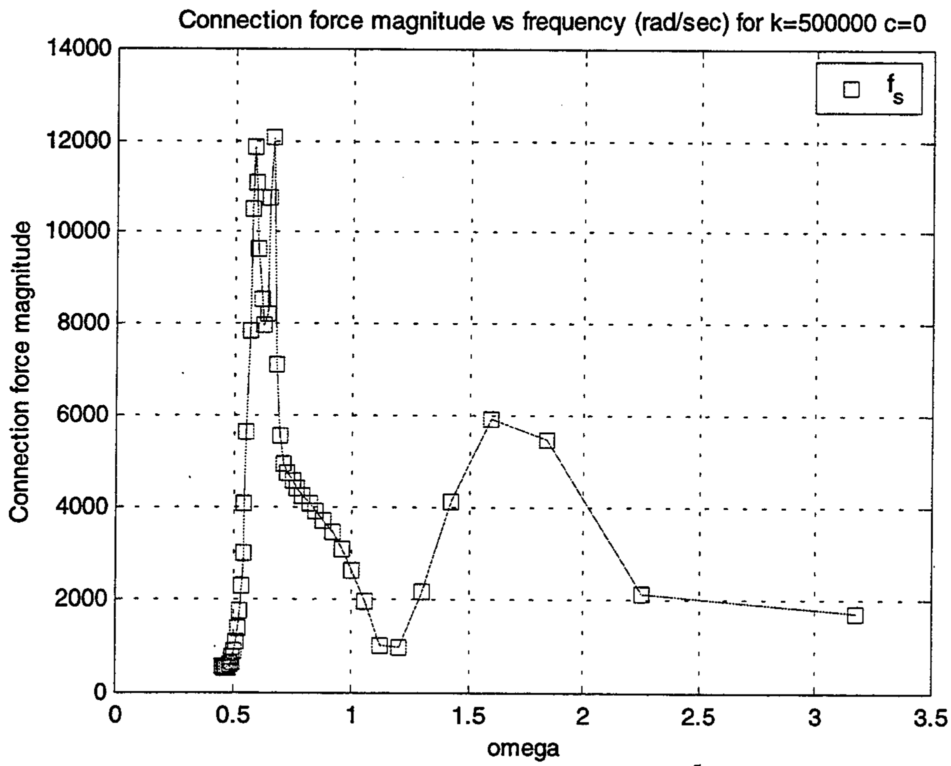

Figure 11. Force magnitude $K=5x10^5$, C=0

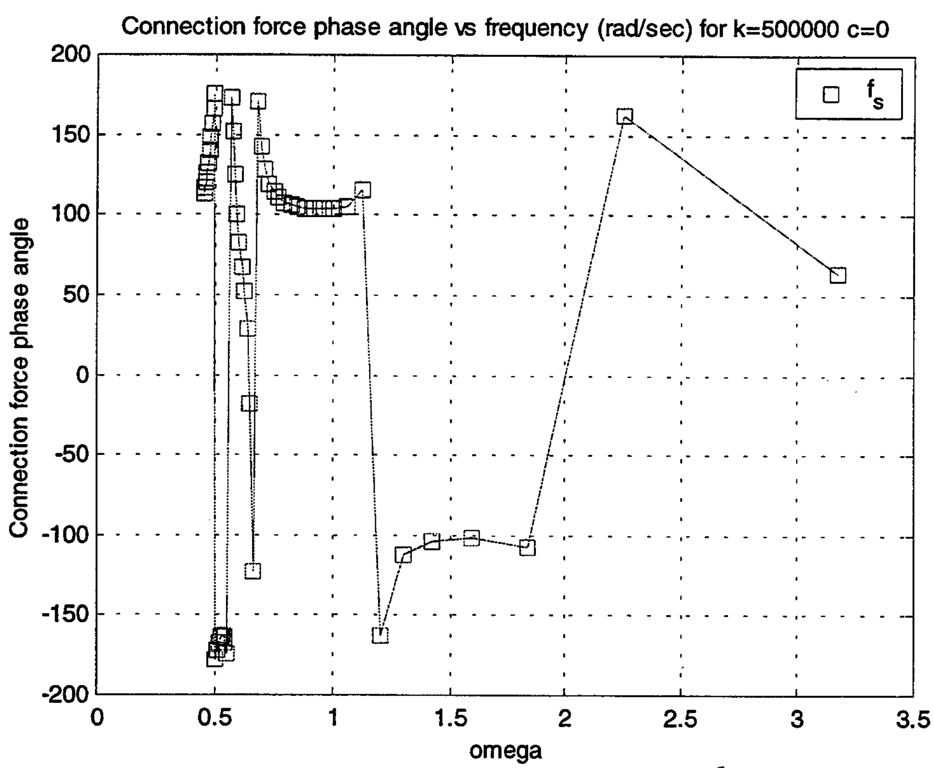

Figure 12. Force phase angle $K=5x10^5$, C=0

4. K=0 lbf/ft; C=5000 lbf-s/ft

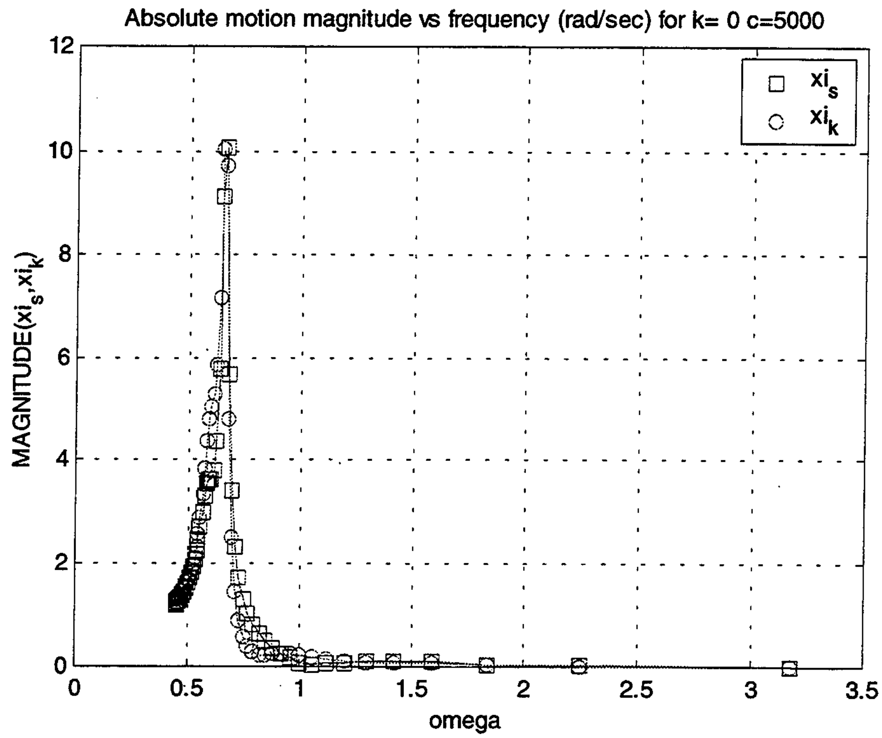

Figure 13. Absolute motion mag. K=0, C=5000

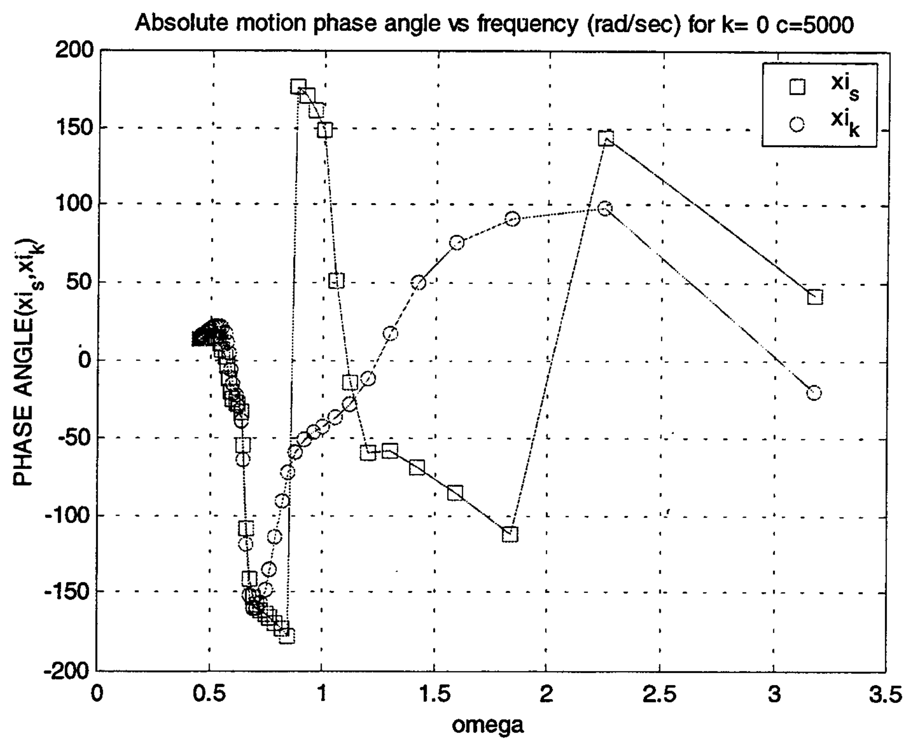

Figure 14. Absolute motion phase K=0, C=5000

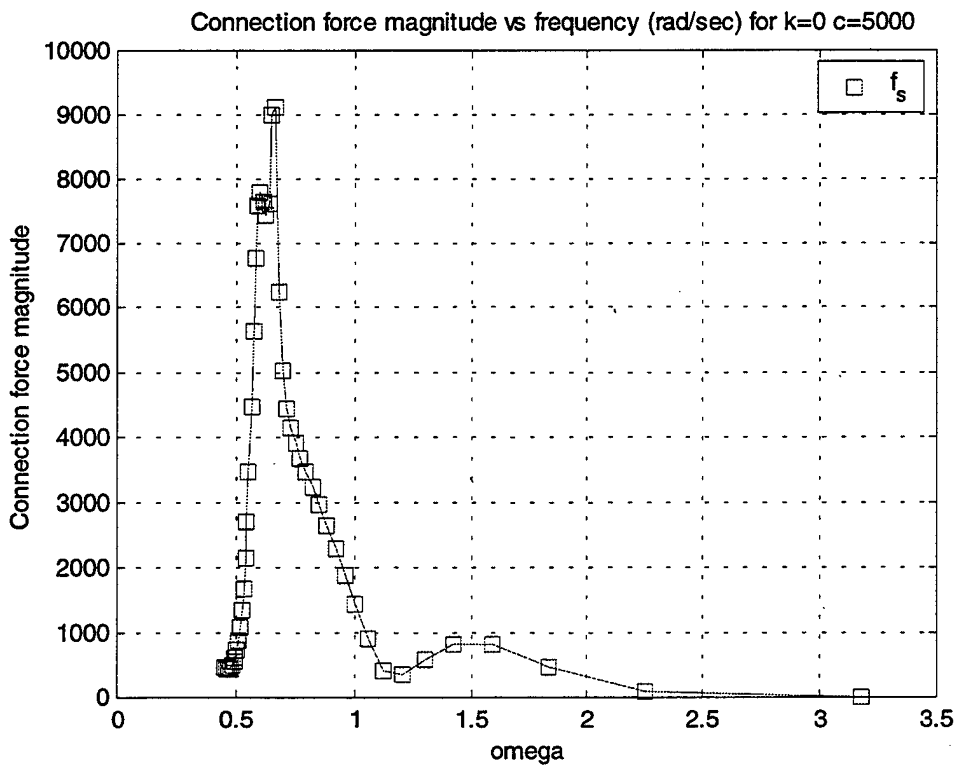

Figure 15. Force magnitude K=0, C=5000

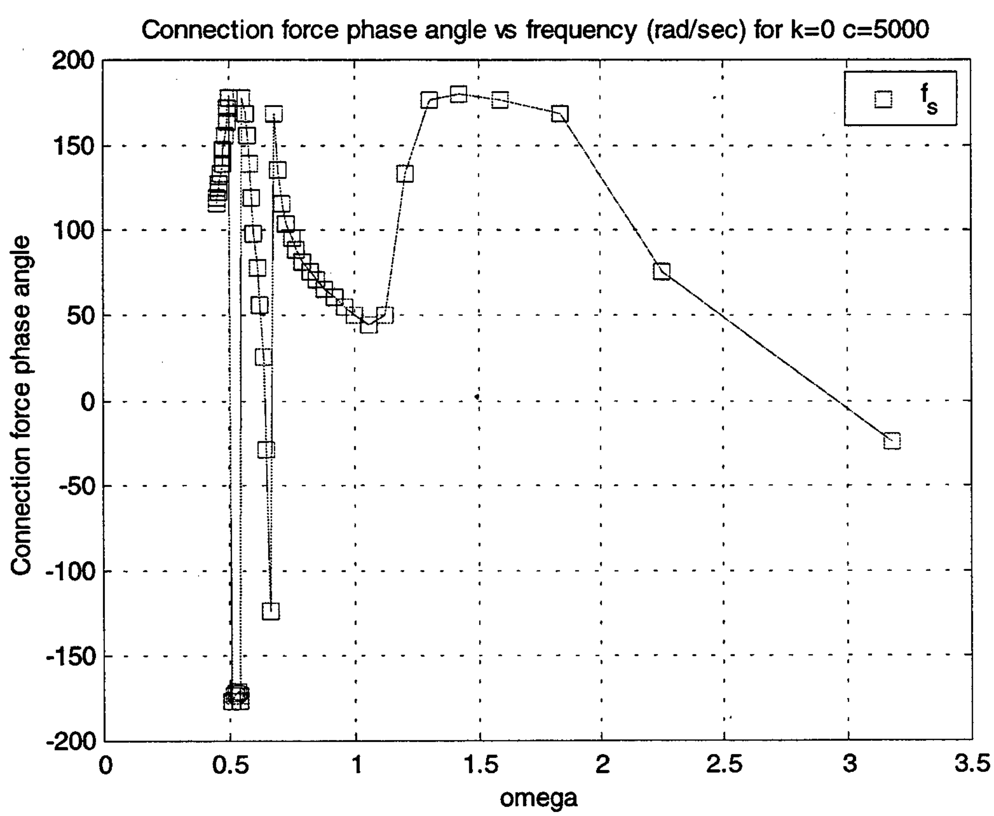

Figure 16. Force phase angle K=0, C=5000

5. K=0 lbf/ft; C=500000 lbf-s/ft

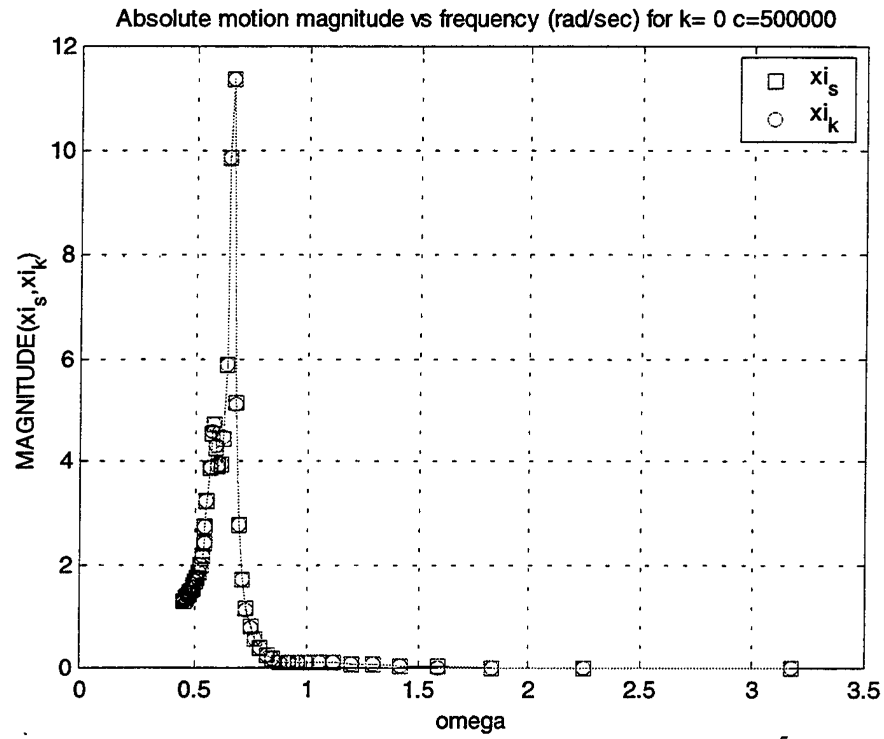

Figure 17. Absolute motion mag. K=0, C=5x10^5

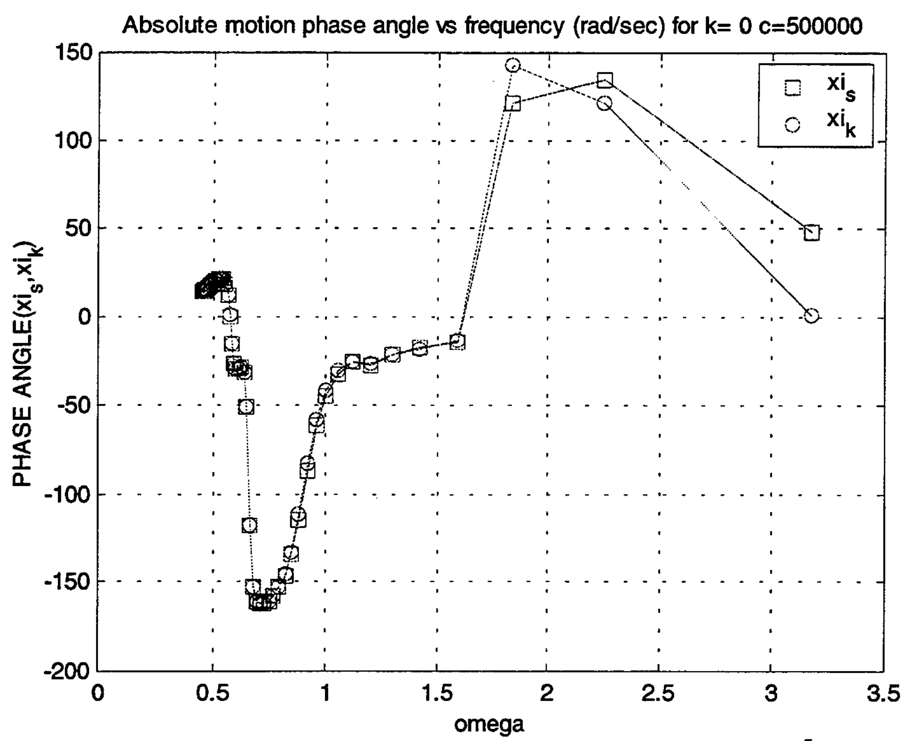

Figure 18. Absolute motion phase K=0, C=5x10^5

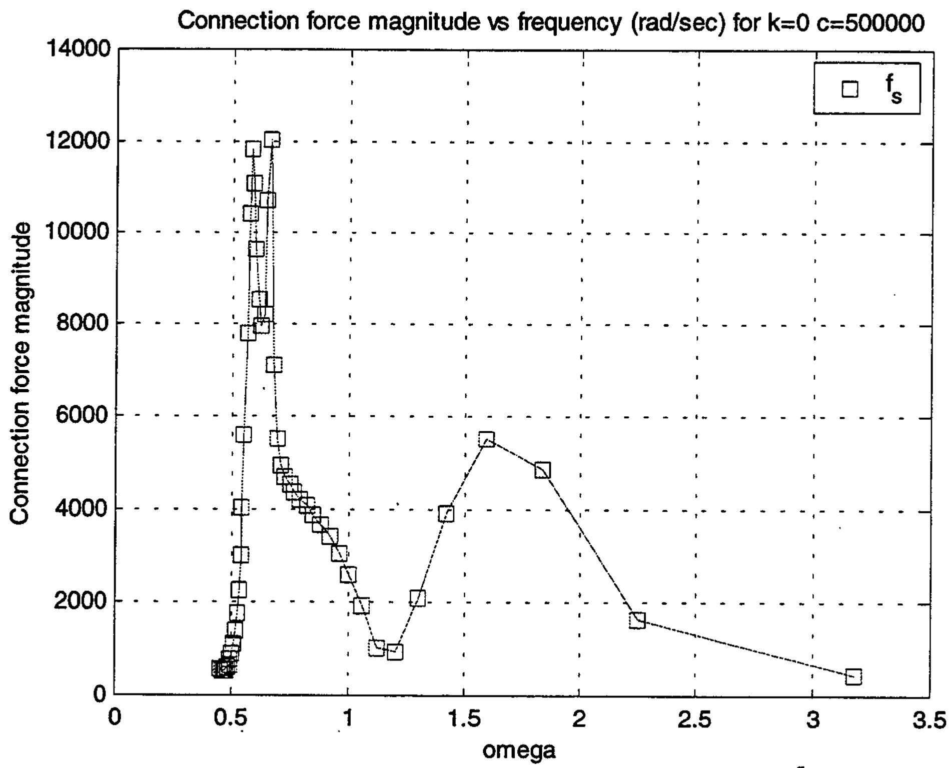

Figure 19. Force magnitude K=0, C=5x10^5

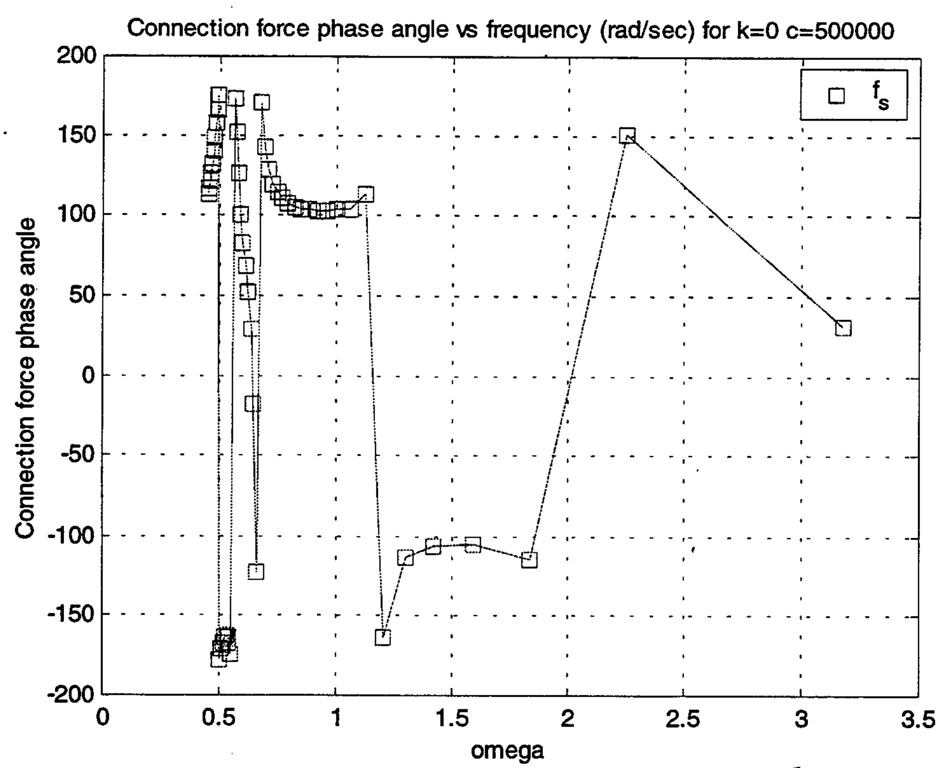

Figure 20. Force phase angle K=0, C=5x10^5

6. K=5000 lbf/ft; C=5000 lbf-s/ft

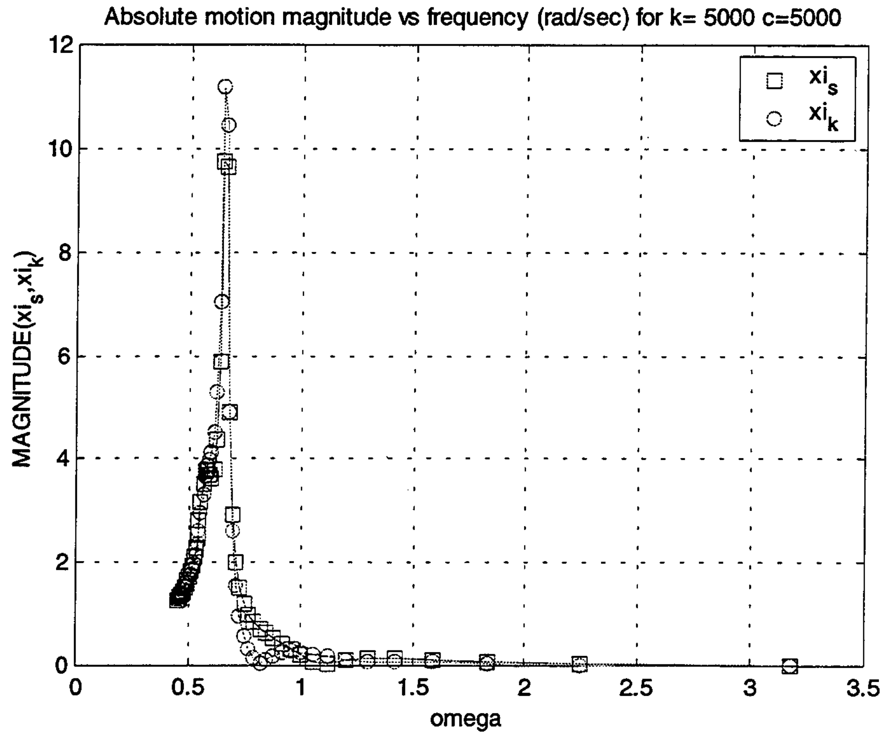

Figure 21. Absolute motion mag. K=5000, C=5000

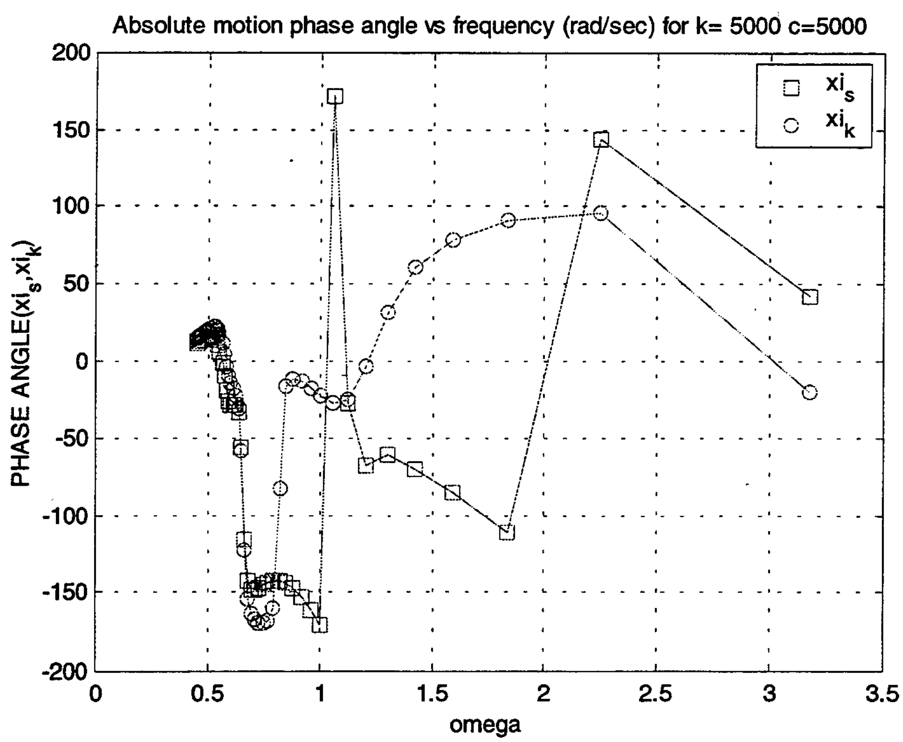

Figure 22. Absolute motion phase K=5000, C=5000

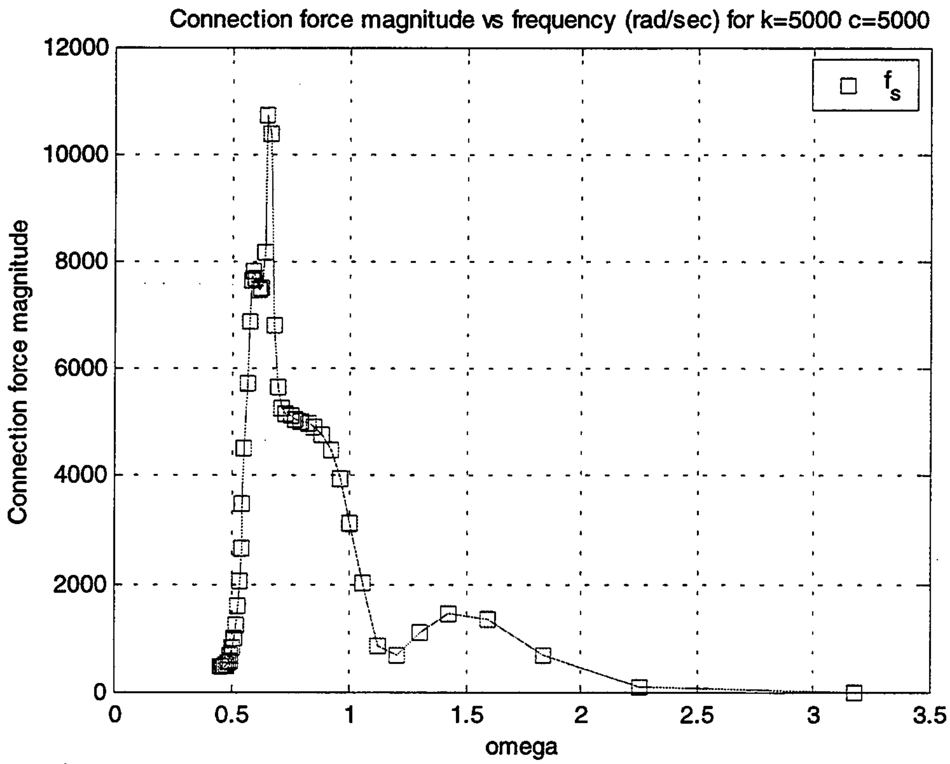

Figure 23. Force magnitude K=5000, C=5000

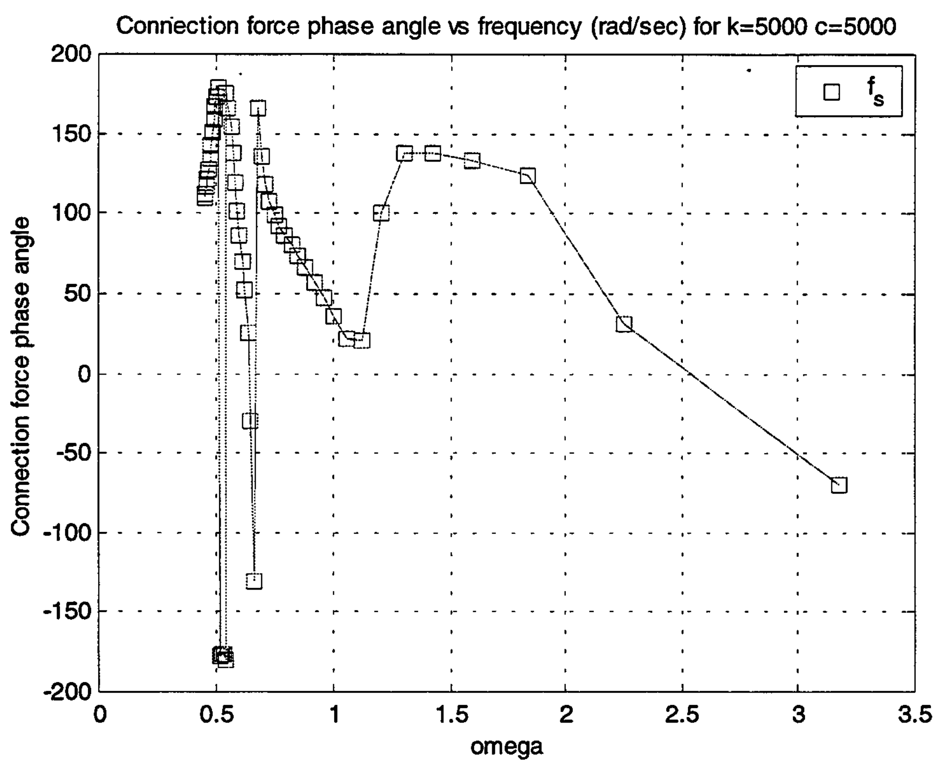

Figure 24. Force phase angle K=5000, C=5000

7. Regular Wave Results Observations

Several fundamental properties of the system are evident in the preceding plots. Figures 2 and 3 show the vessel response for (k=0, c=0). This response is equivalent to two independent vessels in single file, i.e. disconnected. The offset in ω between ξ_s and ξ_k shown in figure (2) is due to the distance separating the connection points. The absolute motion shows resonant peaks for λ = 4-6 times ship length at the example speed and heading. Figure (13) shows the magnitude of these peaks is cut in half as damping is added (c=5000 lb-s/ft). Such peaks evident in regular waves should be substantially reduced in a real seaway because of the random nature of real waves. Furthermore, as would be expected in the disconnected case, figure (4) shows zero connection force for all ω when the spring constant and damping constant are zero.

For average displacement of SLICE and KAIMALINO (~200 tons), as the spring constant is raised to large values relative to the displacement (k=500,000 lb/ft ~ 223 ton/ft), the response of the two vessels approaches that of a single rigid vessel. This behavior is evident in figures (9) and (10), where magnitude and phase angle of the two vessels merge to the same values over the range of ω. A very large damping constant value (c=500,000 lb-s/ft) also models an inflexible connection as shown in figures (17) and (18).

Force and absolute motion magnitude and phase angle, are evaluated to verify the software provides reasonable results. With results verified, the response to any given sea way is now known. Mapping vessel response to seaway motions is the ultimate goal of regular wave models. The function that maps wave input to ship response is the "Response Amplitude Operator", and will be further addressed in random wave analysis.

Plots also provide insight into the variation of force and absolute motion as spring and damping constants are varied. Regular wave modeling program and results are useful tools in the design spiral of an actual towing mechanism. Design trade-offs between minimizing relative motion (large k and c values), and minimizing connection force/tow bar size can be roughly evaluated. Regular wave modeling results are not however, precise enough to base actual design upon. The regular nature of the sinusoidal sea can show false resonance, and abnormally high peak magnitudes that would not be encountered in random seas. To more precisely model vessel response, the response amplitude operator must be mapped to an applicable random sea spectrum.

III. RANDOM WAVE RESPONSE

A. BACKGROUND

1. Spectrum Selection Criteria

A seaway's "spectrum" is a probabilistic function developed by taking the Fourier transform of the correlation function for free surface elevation. (Cummins) The correlation function contains wave height and period data from sources such as buoy observations. The spectrum - $S(\omega)$ – is a measure of the energy contained within a wave system. In a plot of $S(\omega)$ vs. ω, the area under the curve represents the mean energy stored in a particular wave system, $\overline{E} = \int_0^\infty S(\omega)d\omega$.

Numerous wave spectra are available as input for modeling a vessel's operating response to a seaway. Selecting the appropriate spectrum should be accomplished with due regard for the ship's expected operating environment. Environmental conditions such as wind and swell vary geographically, and ship design should be tailored so the vessel responds optimally to the prevailing conditions. Since the environment that SLICE and KAIMALINO will operate is unknown, the *Pierson-Moskowitz* spectrum is chosen. This model predicts the wave spectrum for fully developed, long-crested seas with no underlying swell. Fully developed seas contain waves at equilibrium, independent of fetch and duration of wind. Long crested seas have parallel crests and are assumed to be unidirectional.

The *Pierson-Moskowitz* spectrum is described by

$$S(\omega)=\frac{g^2(8.1x10^{-3})}{\omega^5}\exp\left[-.74\left(\frac{g}{U\omega}\right)^4\right]$$

where: g = gravitational constant

ω = wave frequency (rad/sec)

U = Wind speed at19.5 m above free surface

The above spectrum is dependent on wave frequency and wind speed, a metric the underlying regular wave research does not provide or account for. Regular wave results provide spectral vessel response as a function of frequency for given significant wave height. Correlation between significant wave height and wind speed has been extensively developed, and frequency dependent spectral formulations derived based on significant wave height. (McCreight) Using an empirical relationship between wind speed and wave height, the *Pierson-Moskowitz* spectrum can be predicted using the following relationship:

$$S(\omega)=\frac{8.1x10^{-3}}{\omega^5}\exp\left[\frac{-.032\left(\frac{g}{H_{1/3}}\right)^2}{\omega^4}\right]$$

where: g = gravitational const. (32.2 ft/s^2)

ω = wave frequency (rad/sec)

$H_{1/3}$ = significant wave height (ft.)

Significant wave height is defined as the average of the highest one-third of all wave height observations.

2. Response Amplitude Operator (RAO)

Also known as the motion transfer function, the RAO maps the complex response of a vessel to a seaway or input spectrum as a function of frequency. $S_R(\omega) = |RAO(\omega)|^2 S(\omega)$ Where $S_R(\omega)$ is the response of the vessel to the input sea spectrum for a given frequency. This very powerful relationship allows motions and terms derived from ship motions to be predicted for a given wave frequency and significant wave height. For example, the complex absolute motions predicted in regular wave modeling (ξ_s, ξ_k) are converted into RAO's for absolution motion:

$$RAO(\xi_{s,k}) = abs(\xi_{s,k}).$$

The response spectrum for absolute motion is:

$$S_R\_\xi_{s,k}(\omega) = |abs(\xi_{s,k})|^2 S(\omega).$$

This process may be applied to all motions, and in the case of the close-proximity towing system, the connection force response is:

$$S_R\_f_{connection}(\omega) = |abs(f_{connection})|^2 S(\omega).$$

With the spectral response of a vessel's motion thus determined, the design spiral continues, with random wave results providing a more complete assessment of design objectives. In order to conduct trade-off analysis, or to evaluate performance against changes in environmental, operational, and design parameters, the statistical properties of the response must be determined. In other words, while it is useful to predict the response for a given wave frequency, it is more productive to compare performance over the entire range of the spectrum. A good measure of performance over a range of frequencies is the significant double amplitude of the response. Double amplitudes are obtained by simply integrating the response with respect to frequency over the frequency range of the input spectrum. For instance, the significant double amplitude of the absolute motion of SLICE at the connection point is: $\sigma_{\xi_s} = \int_{\omega_o}^{\omega_f} S_{R\_}\xi_s(\omega) d\omega$.

B. RANDOM WAVE MODELING OF SLICE AND KAIMALINO

1. Process

Regular wave modeling of the SLICE-KAIMALINO integrated tow rig discussed in the previous chapter yields RAO's for absolute motion of both vessels, as well as the RAO for connection force. Using variable forward speeds and wave angles yields RAO's that are functions of the frequency of encounter ω_e rather than actual wave frequency ω. $S(\omega)$ is readily converted to $S(\omega_e)$ because the energy of the seaway will remain constant whether viewed from a stationary point or a moving ship.

$$S(\omega)d\omega = S(\omega_e)d\omega_e \quad \therefore \quad \{energy(\omega) = energy(\omega_e)\}$$

$$S(\omega) = S(\omega_e)\frac{d\omega_e}{d\omega} \quad \therefore \quad \{\omega_e = \omega - \frac{\omega^2}{g}U\cos\beta\}$$

$$\mathbf{S(\omega_e) = S(\omega)[1 - \frac{2\omega}{g}U\cos\beta]^{-1}}$$

The first operation performed in the random wave analysis software is defining the *Pierson-Moskowitz* spectrum and transforming it as shown above. Next, the response spectra are defined. The most interesting response in determination of feasibility of the close-proximity towing system is the connection force, whose response spectrum is defined as $S_f(\omega_e) = \left|abs(f_{connection})\right|^2 S(\omega_e)$.

Integration of the connection force response spectrum, $\sigma_{fconn} = \int_{\omega_{eo}}^{\omega_{ef}} S_f(\omega_e) d\omega_e$

is accomplished numerically by summing the product in the integrand of the preceding integral. In other words,

$$\sigma_{fconn} = S_{f,(0)} + \sum_{i=1}^{\#of\,\omega's} (S_{f,(i)} + S_{f,(i-1)})(\omega_{e,(i-1)} - \omega_{e,(i)}) \,.$$

The resultant σ_{fconn} is now transformed to significant double amplitude, $\sigma_f = 4\sqrt{\sigma_{fconn}}$. The significant double amplitude represents the average of one third of the highest probable connection forces encountered for the given input condition in waves with wavelength from twenty to one thousand feet.

2. Results

The random wave simulation described above adds significant wave height to the list of input parameters that were varied in the regular wave studies. Recall that a database of regular wave RAO's for both SLICE and KAIMALINO was created, for speeds from zero to 20 knots, and wave angles from 0° to 180°. Combining the database, regular wave simulation, and random wave simulation enables parametric studies to be conducted. Several questions should be answered before the tow mechanism is designed. Is the connection force in seas up to sea state five small enough to make integrated connection feasible? If the force is manageable, what spring and damping constants should be used to minimize the force? And finally, which sea directions and ship speeds drive connection force to unacceptably large values?

Armed with random seas software, these questions are researched by varying ship speed, wave angle, significant wave height, and spring-damper constants. Standard values are used throughout to allow cross-reference between plots. Standard speed is 15 knots, wave angle is 45°, significant wave height is 5 feet, and spring and damper constants are set to zero. Similarly, when each parameter is varied, it must be done so in a like manner from one run to the next. Standard parameter variations are:

V	0—15 kts	Every 3 knots
β	0—180°	Every 30°
$H_{1/3}$	0—10 ft	Every tow feet
C and K	1—100,000 lb-s/ft K in lb/ft	Eight values evenly spaced on log scale from 10^0 to 10^5

Table 2. Parametric Variations

Using these parameter variations, random wave simulations are run and connection force is calculated as a significant double amplitude (σ_f). Connection force is selected as the common metric against which all variables are compared. Similar parametric studies can be run using absolute motion (ξ_s, ξ_k) as the dependent comparison variable. Plotting σ_f versus V, β, k, and c reveals optimum values of each of the variables for minimizing significant connection force. Finally, the plots provide a tool for design of the actual close-proximity towing mechanism. The optimum spring-damper values and maximum expected connection force output by the random wave simulation provide the basis for solid mechanics engineering of the tow bar. For instance, with maximum σ_f as the design force, maximum yield stress and Euler buckling theories might dictate the cross-sectional parameters of the tow bar. Such a case study is presented in the next chapter.

a. $\sigma_{f\,(lbf)}$ ***versus*** $H_{(1/3)\text{-}ft}$

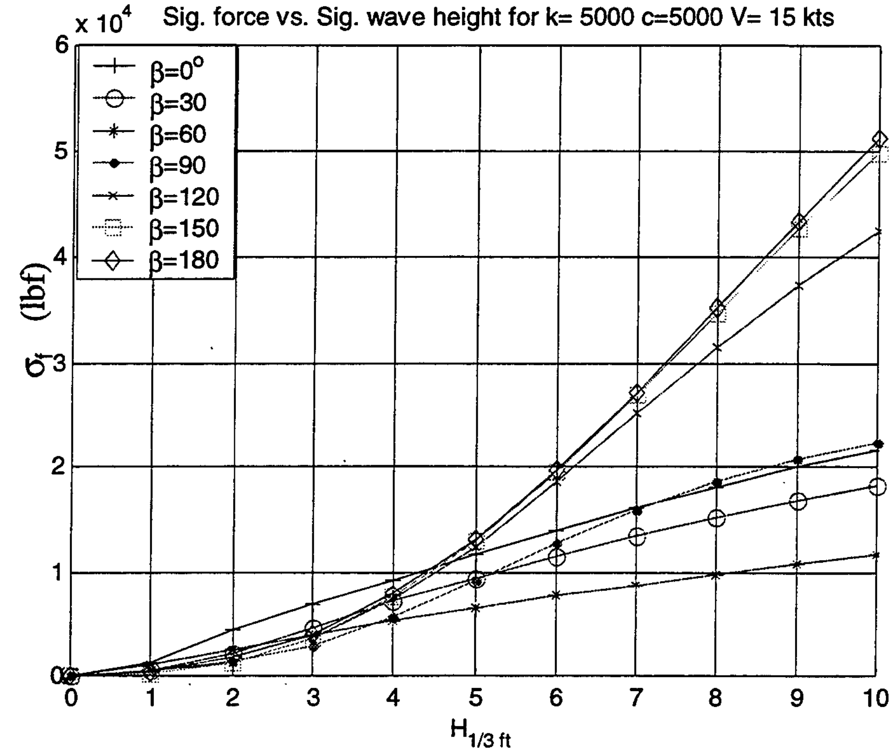

Figure 25. Force vs. $H_{(1/3)}$, (β varied)

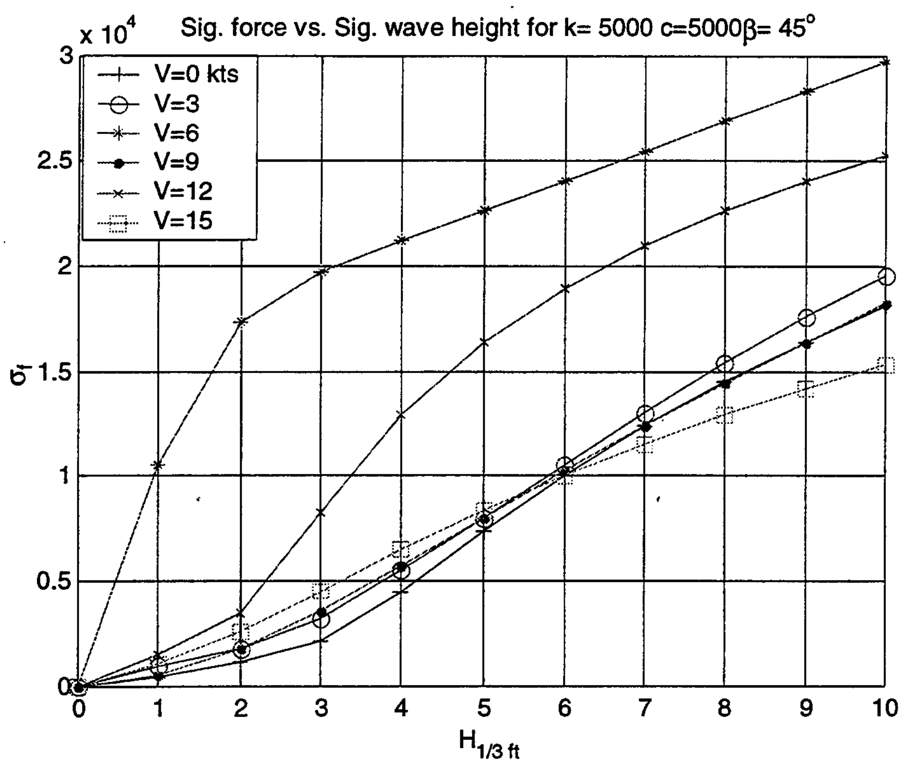

Figure 26. Force vs. $H_{(1/3)}$, (V varied)

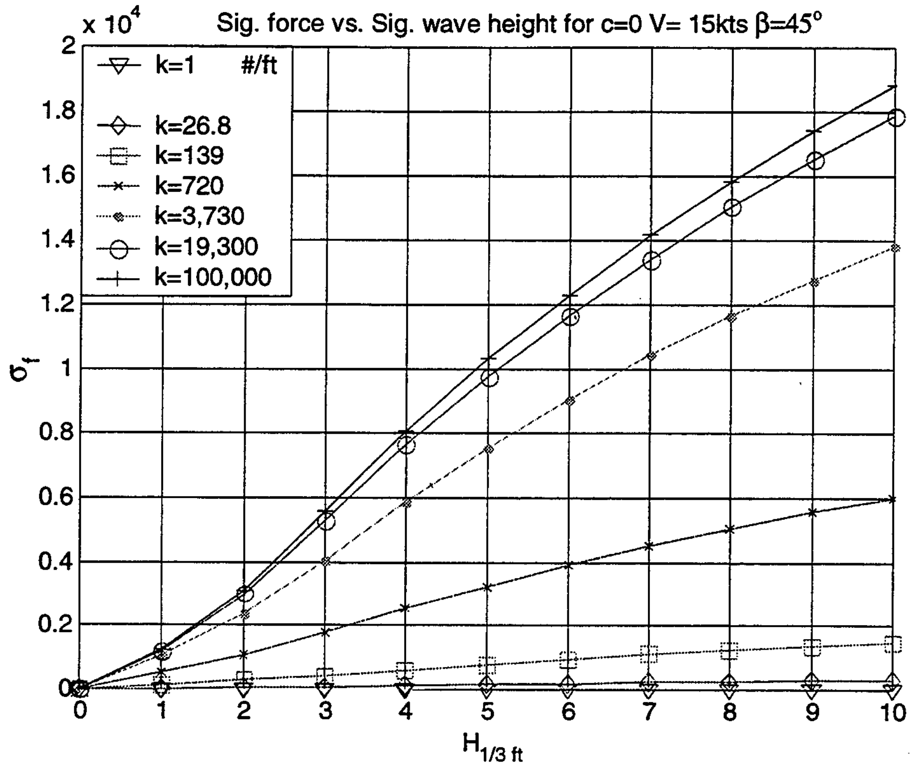

Figure 27. Force vs. $H_{(1/3)}$, (k varied)

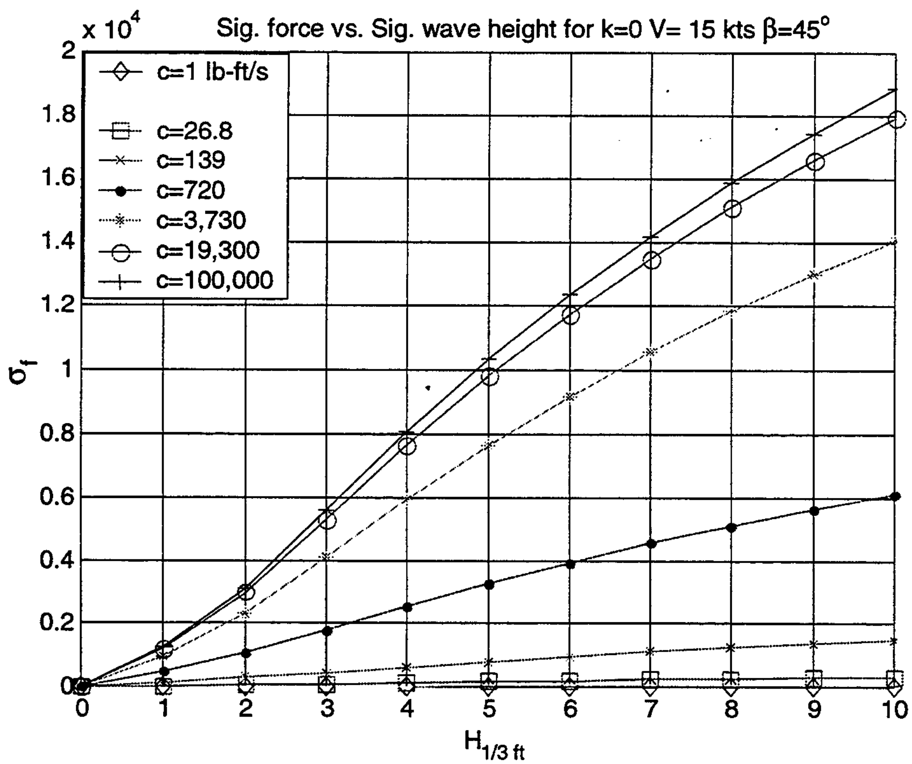

Figure 28. Force vs. $H_{(1/3)}$, (c varied)

b. $\sigma_{f\,(lbf)}$ versus V_{kts}

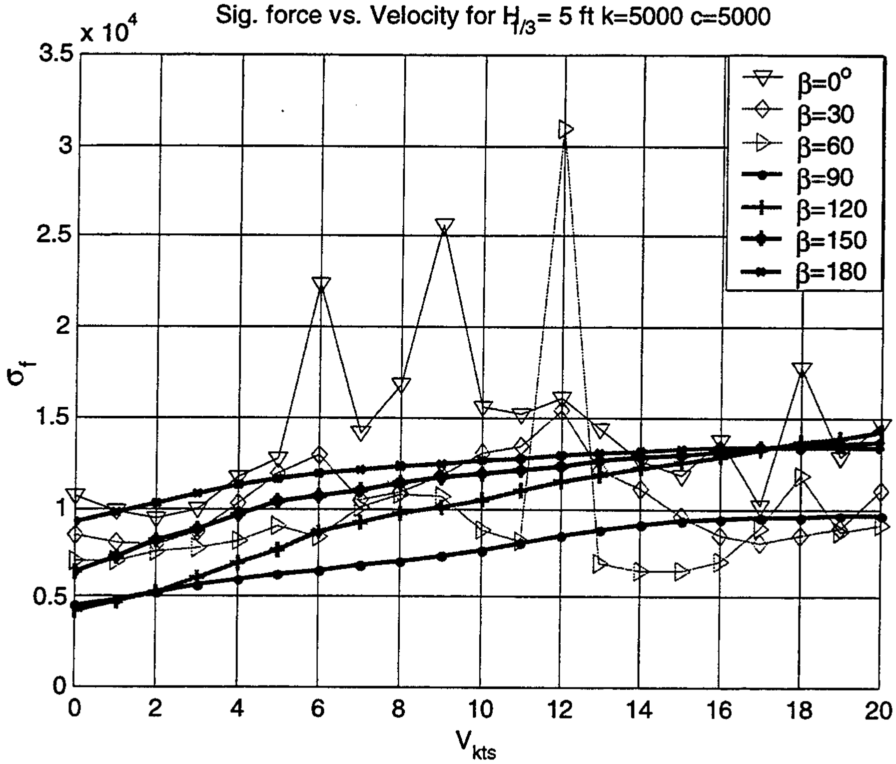

Figure 29. Force vs. V_{kts}, (β varied)

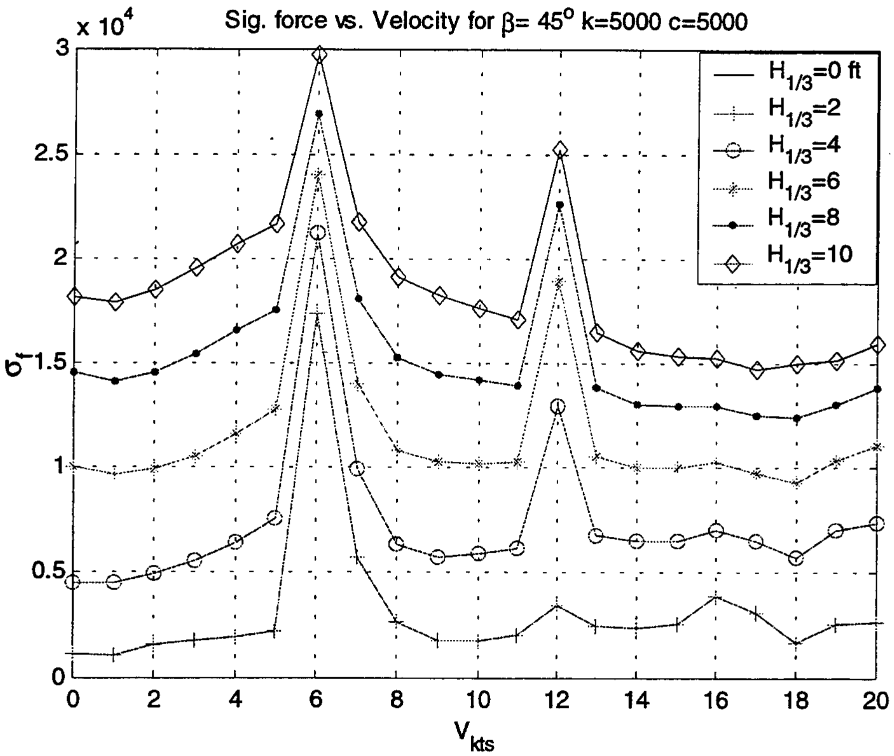

Figure 30. Force vs. V_{kts}, ($H_{1/3}$ varied)

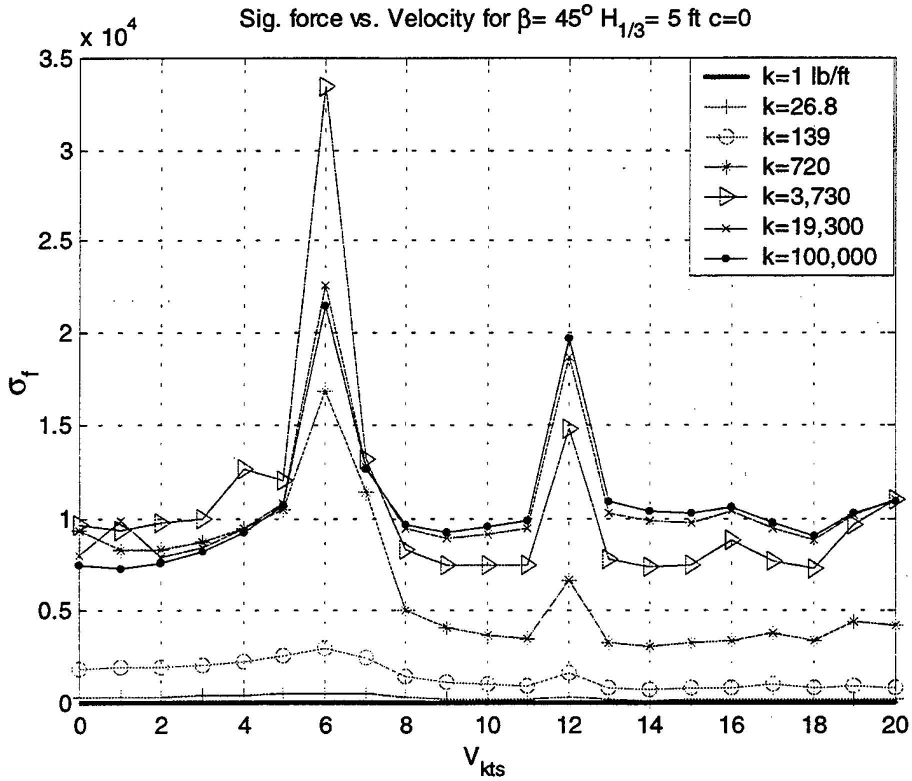

Figure 31. Force vs. V_{kts}, (k varied)

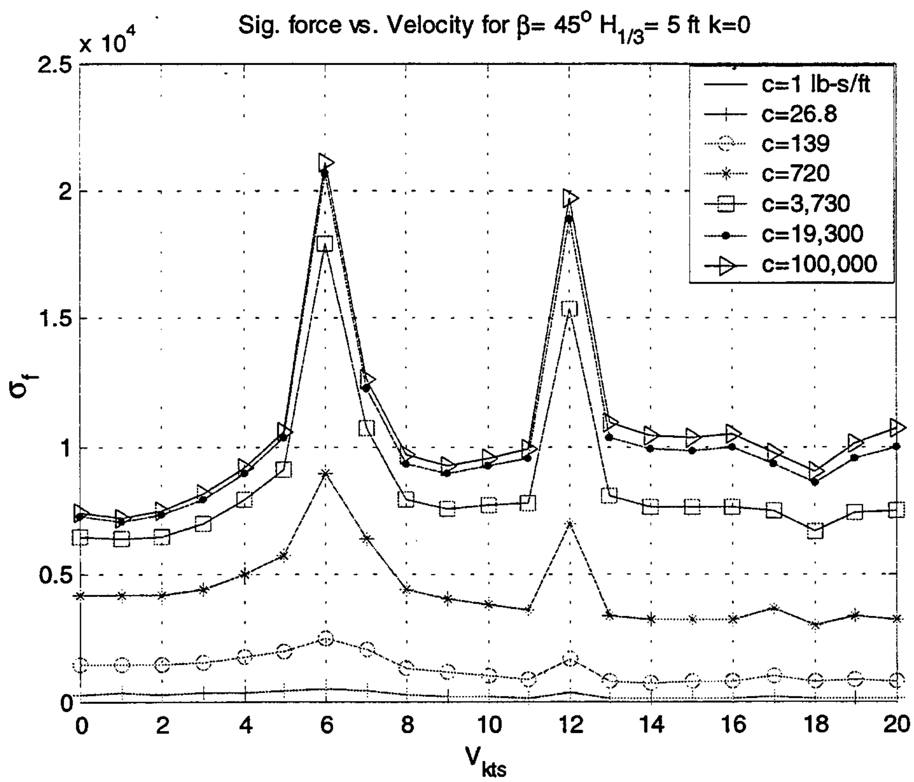

Figure 32. Force vs. V_{kts}, (c varied)

c. $\sigma_{f\,(lbf)}$ versus $\beta_{degrees}$

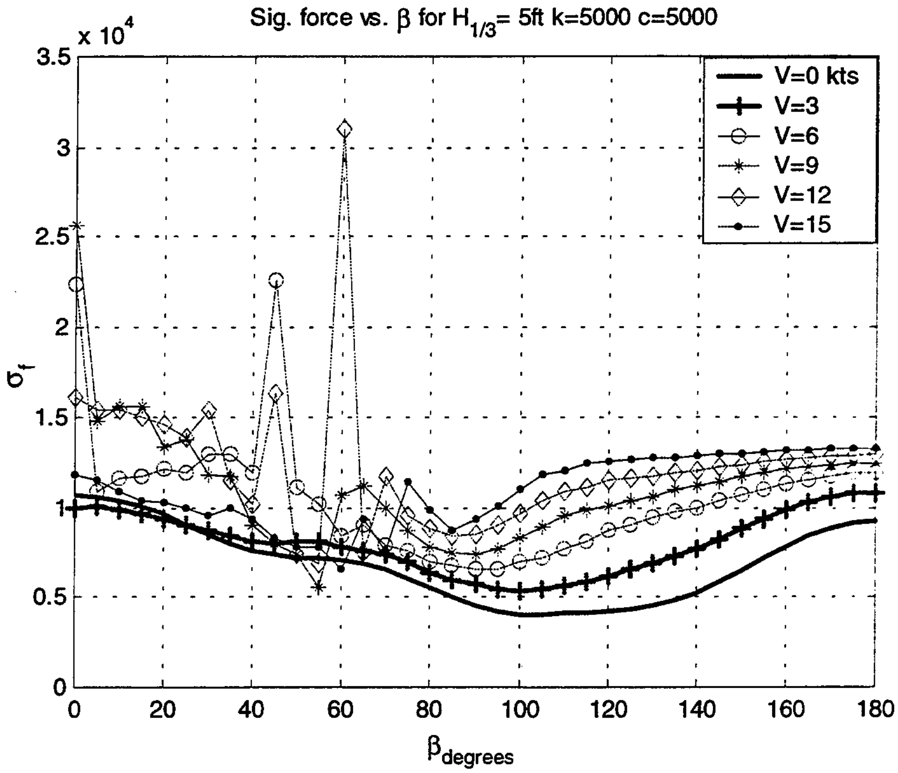

Figure 33. Force vs. $\beta_{degrees}$, (V varied)

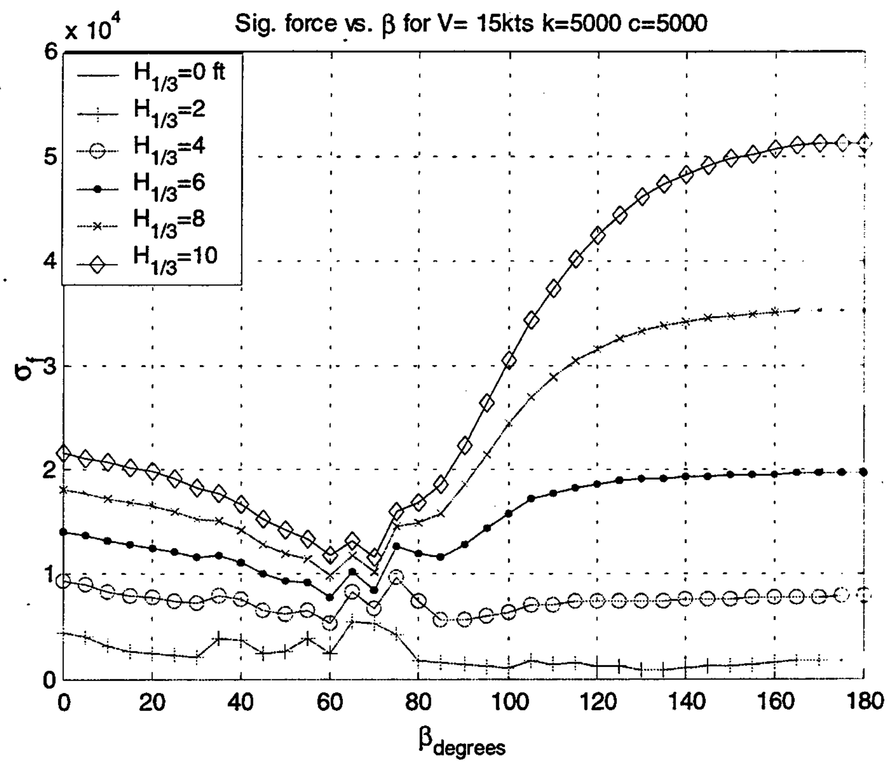

Figure 34. Force vs. $\beta_{degrees}$, ($H_{(1/3)}$ varied)

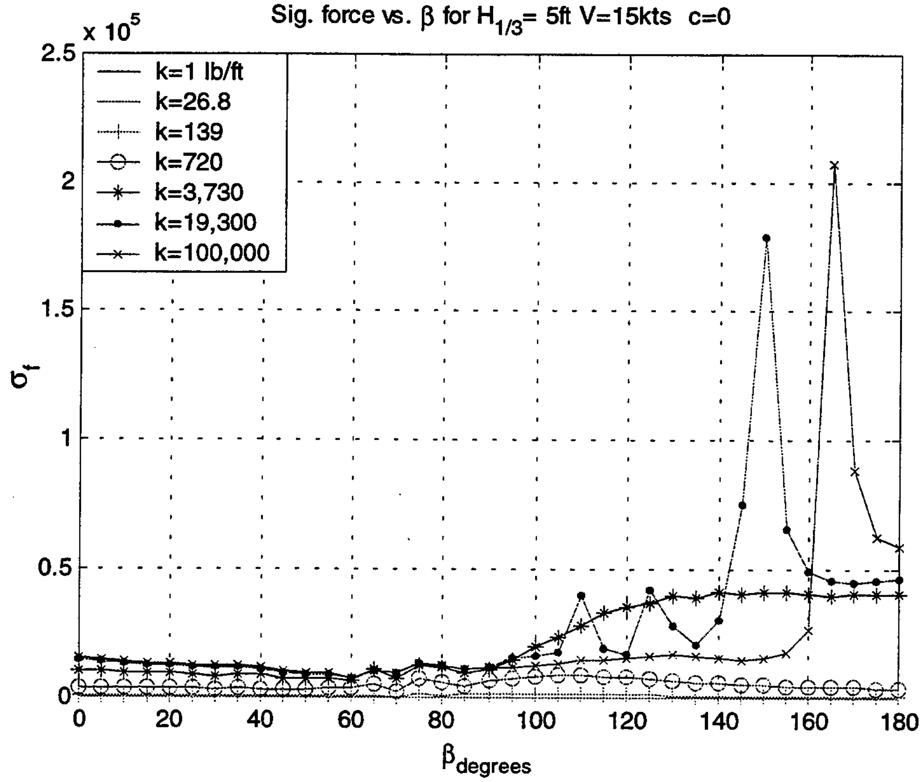

Figure 35. Force vs. $\beta_{degrees}$, (k varied)

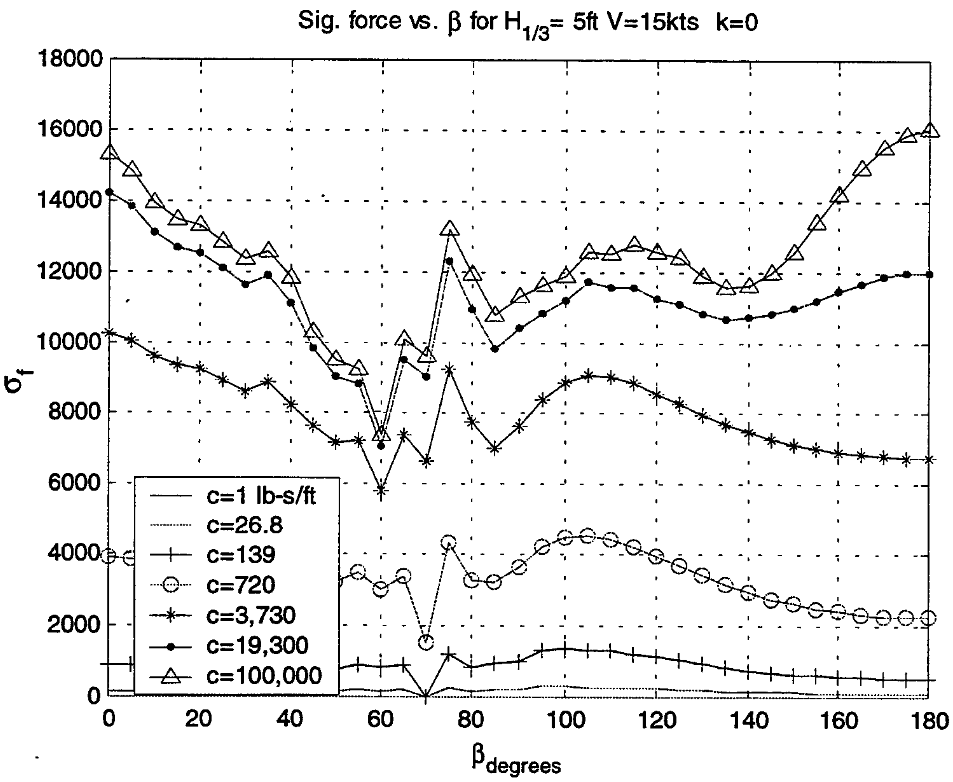

Figure 36. Force vs. $\beta_{degrees}$, (c varied)

d. $\sigma_{f\,(lbf)}$ versus $K_{lbf/ft}$

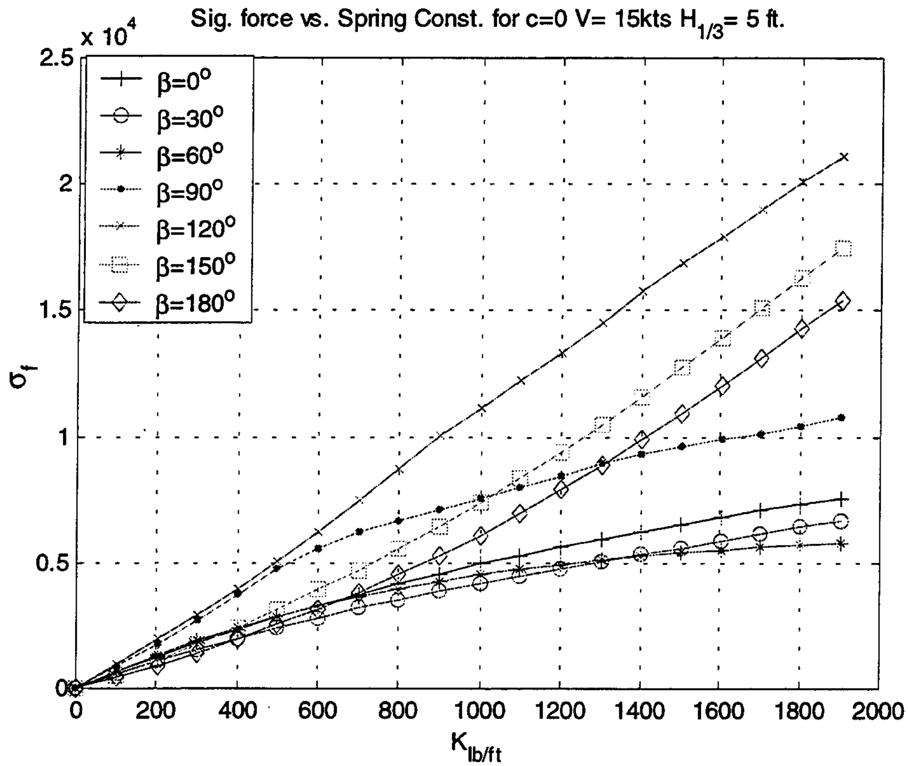

Figure 37. Force vs. $k_{lb/ft}$, (β varied)

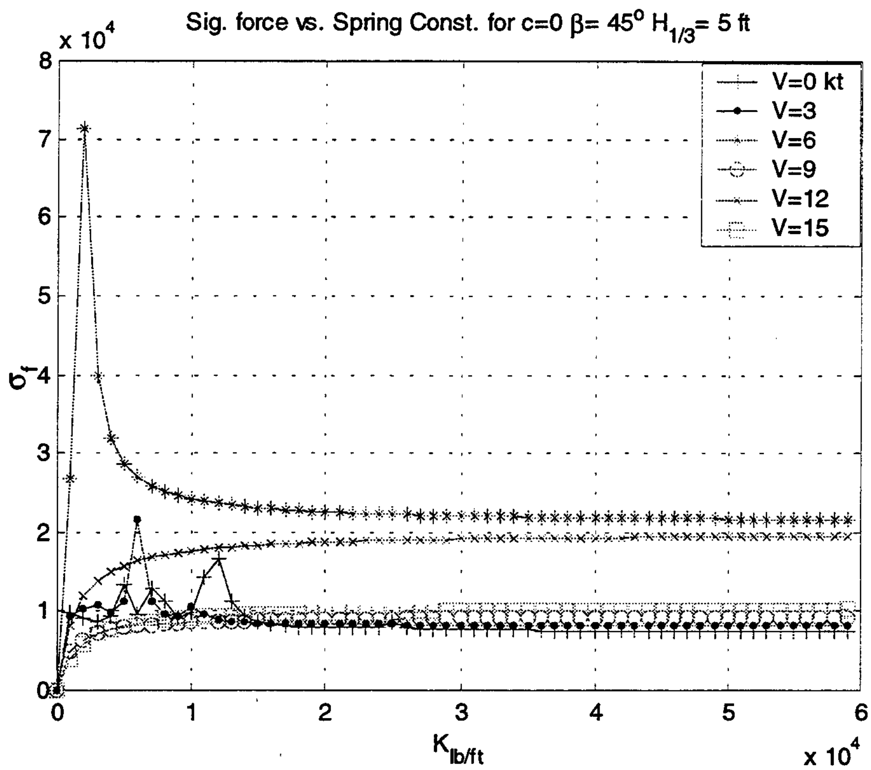

Figure 38. Force vs. $k_{lb/ft}$, (V varied)

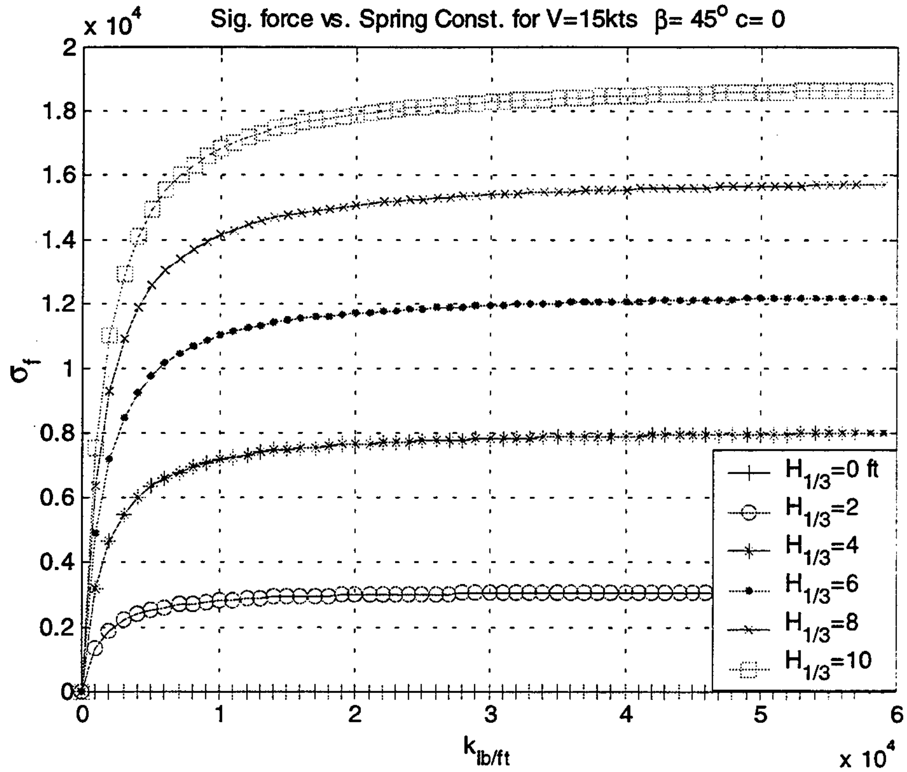

Figure 39. Force vs. $k_{lb/ft}$, ($H_{(1/3)}$ varied)

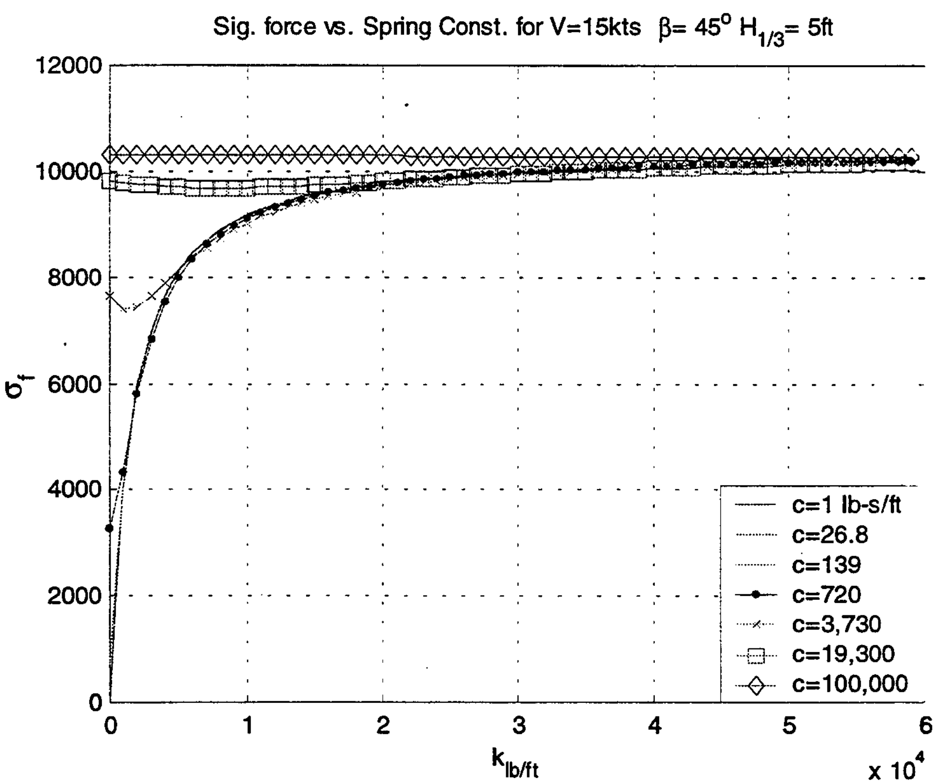

Figure 40. Force vs. $k_{lb/ft}$, (c varied)

e. $\sigma_{f\,(lbf)}$ ***versus*** $C_{lbf\text{-}s/ft}$

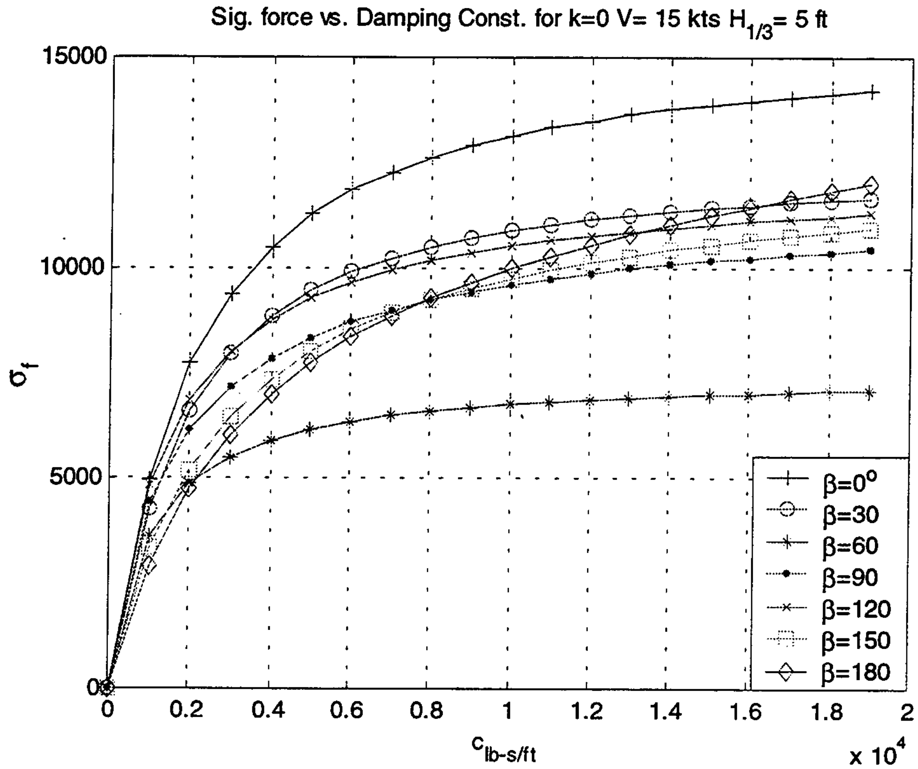

Figure 41. Force vs. $c_{lb\text{-}s/ft}$, (β varied)

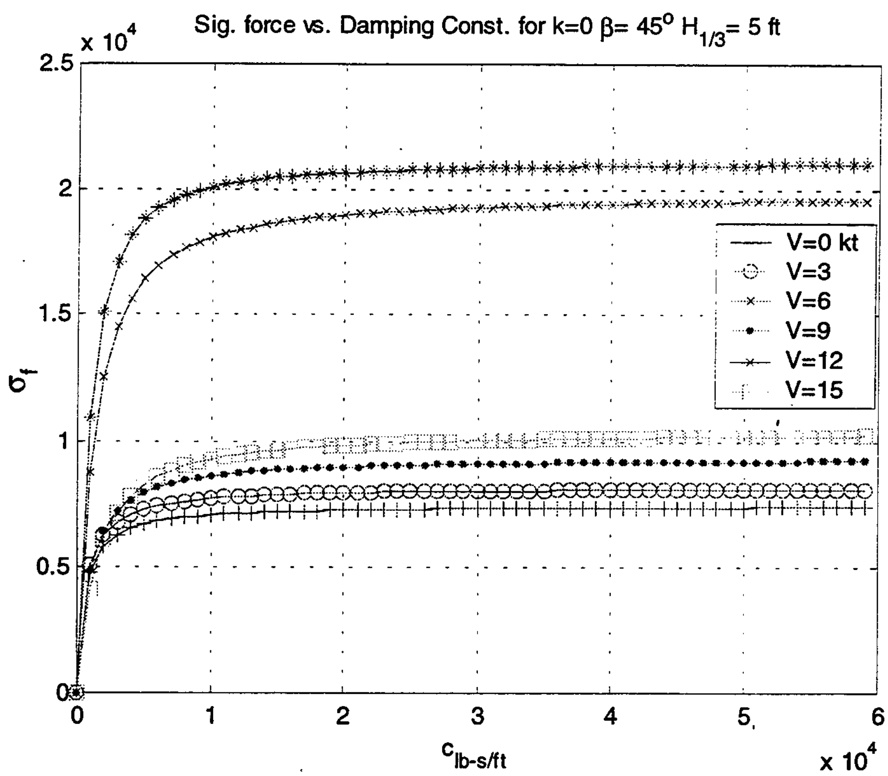

Figure 42. Force vs. $c_{lb\text{-}s/ft}$, (V varied)

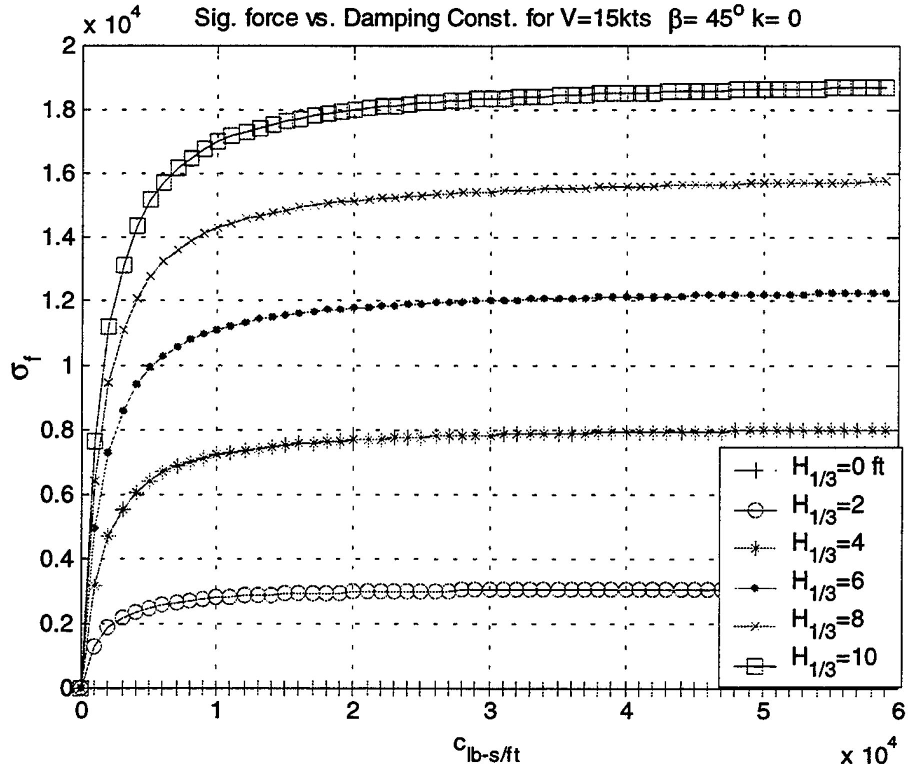

Figure 43. Force vs. $c_{lb\text{-}s/ft}$, ($H_{(1/3)}$ varied)

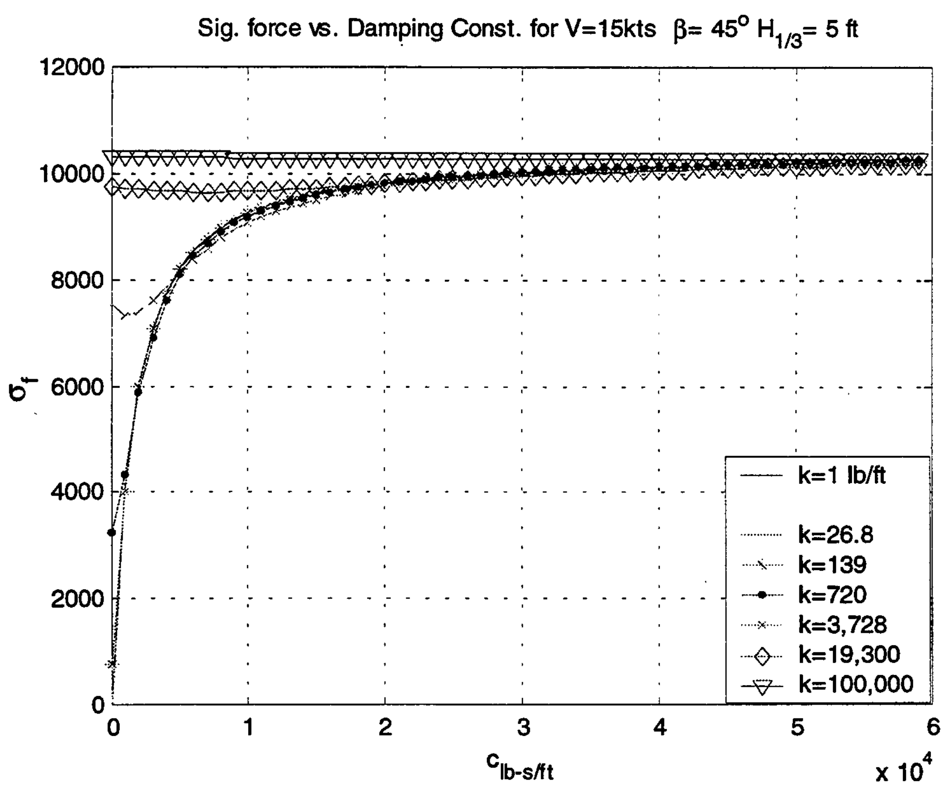

Figure 44. Force vs. $c_{lb\text{-}s/ft}$, (k varied)

3. Seakeeping Evaluations

Variation in connection force double amplitude with significant wave height provides largely intuitive results. Figure 27 shows a linear rise in connection force as significant wave height increases from zero to ten feet. Increasing the spring constant values from 1 lb/ft to 100,000 lb/ft is equivalent to raising the rigidity of the connection from disconnected to rigidly connected. As expected, the connection force rises as the connection becomes more rigid. The slope of the σ_f versus $H_{(1/3)}$ increases as spring constant values increase. A similar phenomenon is evident in figure 28 where connection force amplitude rises with wave height, for all values of damping constant, and the slope of the rise increases with damping constant increase.

Forward speed and wave angle variations reveal several interesting results. Figure 25 shows higher connection force for following seas ($\beta<90^\circ$) than head seas for wave height less than four feet. However, as significant wave height increases from four to ten feet, the slope of the head seas cases immediately rises, yielding much higher connection force for the head seas case at a ten foot wave height. The most interesting results shown in figure 26, the σ_f versus $H_{(1/3)}$ plot for various speeds are the high connection forces corresponding to speeds of three, six, and twelve knots. Six knots yielded the highest connection force, with twelve and three knots being next in line. The effects of speed and wave angle on connection force are reaffirmed in the σ_f versus V and σ_f versus β plots. Figures 30, 31, and 32 clearly show the six and twelve knot force peaks. Figure 34 confirms the much higher connection force for following than head seas. It is important to note however, that the connection force used in analysis was developed from vertical plane motions only. Transforming the simulation to include surge forces is likely to raise the magnitude of the connection force in following seas.

The relationship between spring-damper constants and connection force is perhaps the most useful in design of the towing mechanism. Force dependence on wave height, wave angle, and speed provide operating characteristics of the integrated vessels, and result in engineering and operating limits due to environmental factors. For the design in question, the only remaining variables that can be manipulated by engineers to minimize the connection force are the spring-damper constants. Evaluation of the parametric plots of σ_f versus k and σ_f versus c reveals optimum spring and damping constants to minimize connection force. For instance, figures 40 and 44 show that for values of spring and damper constants in the two to three thousand lb/ft and lb-s/ft range the connection force drops to values less than 8000 pounds, while providing adequate rigidity. Follow on structural design of the tow member can be accomplished by iterating the spring-damper constants in this region for significant connection force and absolute motion to meet designer specifications.

IV. SAMPLE TOWING DESIGN

A. NOTIONAL ARCHITECTURE

Several notional towing mechanisms have been introduced by Lockheed-Martin Marietta for possible design in the integrated SLICE-KAIMALINO project, and several features are common to each design. As discussed in chapter I, forces on the tow rig are due to the difference in motion of the two vessels. A hybrid design was developed for the NPS Total Ship Systems Engineering SEA-LANCE high-speed patrol craft and grid deployment module. This design attempts to minimize the number of degrees of freedom constrained, while also simplifying control architecture and tow mating in the open ocean.

Figure 45 shows a notional close-proximity towing design. This design minimizes connection forces by constraining only those degrees of freedom necessary to provide control and stability in adverse sea states. The most severe motions in a sea way are expected to be in the form of roll, pitch and yaw. To minimize handling equipment size these motions are unconstrained between the SLICE and KAIMALINO in the tow bar. Yaw is constrained at the bow of the KAIMALINO only by "moment cables that prevent jackknifing. Surge is constrained by the tow bar, while sway is limited by the directional stability of KAIMALINO's SWATH hull and constant tension winches that could be mounted at the forward outermost edges of KAIMALINO's bow. Hinges that decouple pitch at both the KAIMALINO and SLICE extremities minimize heave forces. Finally, roll is decoupled between KAIMALINO and SLICE by a roll bearing at the stern of SLICE.

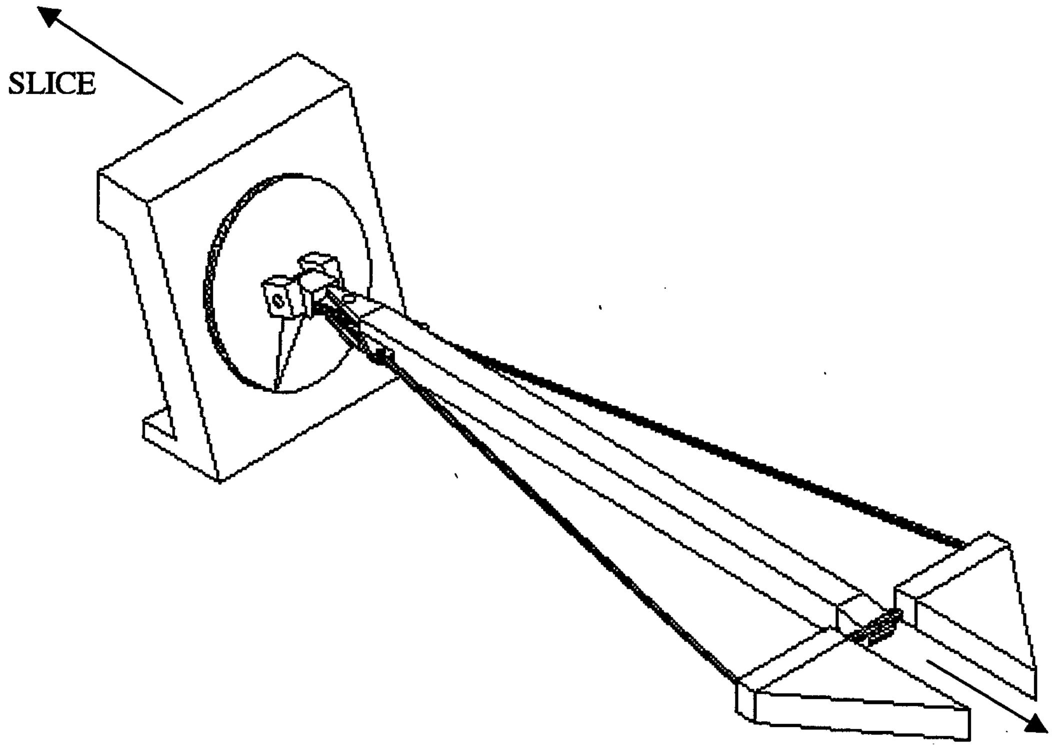

Figure 45. Notional Tow Connection

B. DESIGN APPROACH AND RESULTS

1. Operating Environment and Assumptions

Design of a notional towing system is accomplished by using simulated connection force outputs to analytically calculate stresses at critical locations in design. Geometric and force magnitude considerations dictate tow bar length. Several stress analysis techniques will then be used to determine the minimum cross-sectional size of load bearing components.

The design approach and outcome are heavily influenced by simulation and analytical limitations of the research. For instance, only vertical absolute motions are simulated, so sizing of the tow bar and equipment is based on peak vertical forces expected at a transit speed of 15 knots. Peak vertical connection forces were discovered in the previous chapter to exist in head seas. The operating environment evaluated ($\beta=180^{\circ}$), is expected to result in the highest connection forces for a given sea state at 15 knots.

Next, the spring-damper constants optimized in the random wave analysis must be modeled to predict the interaction between SLICE and KAIMALINO. Recall the equations of absolute motion describing the connection force

$$f=k(\xi_s-\xi_k)+c(\dot{\xi}_s-\dot{\xi}_k)\rightarrow \textit{time domain}$$
$$f=(k+ic)(\xi_s-\xi_k)\rightarrow \textit{frequency domain}$$

The damping constants are difficult to model without knowledge of the exact characteristics of the joint rotations and are assumed to be zero. The vertical connection force however is controlled by the tension between the vessels and the amount of vertical displacement separating them. As such, the spring constant value may be modeled as $k=T/L_{tow}$, where T is tension in the tow bar due to hull resistance obtained from resistance versus speed curves of KAIMALINO, and L_{tow} is the length of the tow bar. Notice that the spring constant decreases with tow bar length. Geometric considerations dictate that tow bar must be long enough to prevent impact of SLICE and KAIMALINO during maneuver. While connection forces drop as length increases, bar rigidity decreases and is more prone to buckling. Additionally, bar length should be minimized to increase integrated towing maneuverability.

2. Random Sea Modeling

Random seas modeling developed in the previous chapter is the basis for connection force determination and subsequent handling gear sizing requirements. Spring constants in the modeling software are set to $k=T/L_{tow}$, and connection forces are evaluated for lengths from 10 to 20 feet. For a forward speed of 15 knots, KAIMALINO resistance (T) is 35,000 pounds. Figure 46 shows the rise in connection force as significant wave height increases and tow bar length decreases.

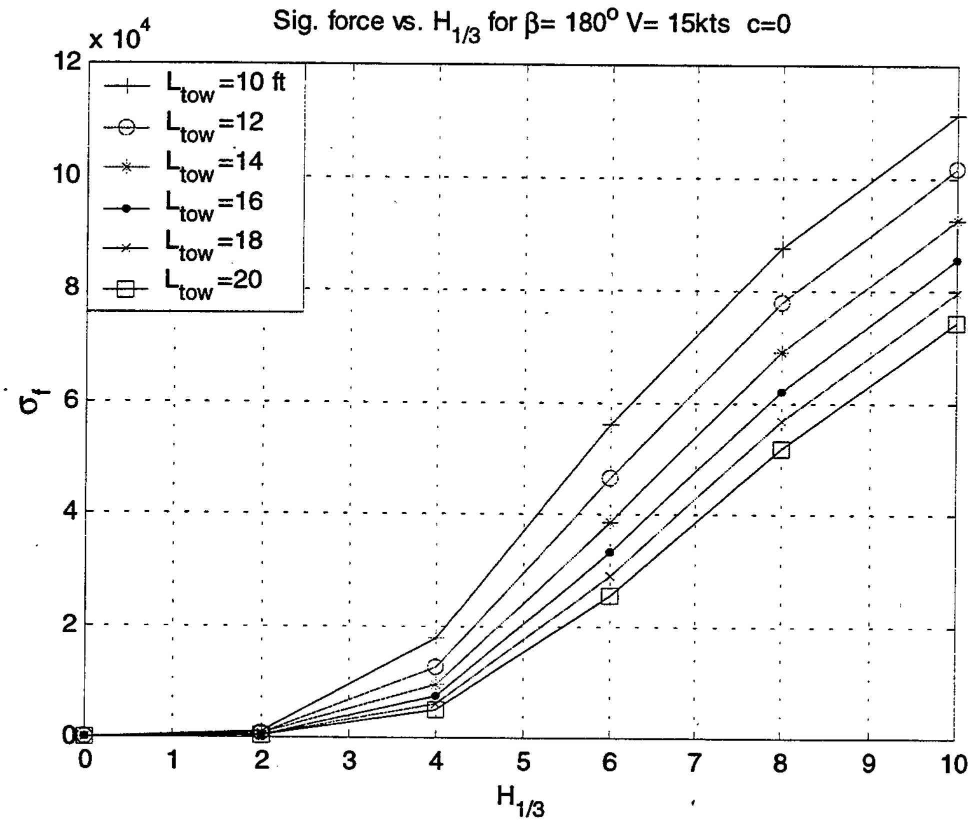

Figure 46. σ_f vs. $H_{(1/3)}$, ($k=T/L_{tow}$)

To minimize connection force and allow rotational freedom up to 45°, the tow bar length is chosen as L_{tow}=20 feet. As a result, for 10-foot seas, the maximum vertical force on the tow bar will be 79,000 pounds.

3. Stress Evaluation and Component Sizing

Assumed forces include: forces from seaway and hydrodynamic resistance. Each of these forces results in a stress on the tow system. Three structural limitations are considered; Euler buckling, static yield stress, and shear yield stress.

Seaway forces are derived from strip theory for a given tow bar length. The primary forces of concern are the vertical force applied to the tow bar both in compression and tension, and the towing resistance. $F_l \cos(\phi) = T$ F_l is the axial resultant force in the tow bar, and ϕ is the angle formed due absolute vertical motion between SLICE and KAIMALINO. For a max expected pitch angle of 25°, and towing resistance of 35,000 pounds at 15 knots, F_l=38,618 pounds. For an assumed box beam with outer diameter of 8 inches, F_l is used to calculate tow bar thickness, (t=0.34 inches) using basic buckling and static yield stress analysis as follows.

Buckling: $$F_l(safetyfactor) = \frac{\pi^2 EI}{Le^2} \qquad I = \frac{1}{12}(s_o{}^4 - s_i{}^4)$$

Yield stress: $$F_l(safetyfactor) = \sigma_y(s_o^2 - s_i^2)$$

Where: Esteel=29,000 psi; safety factor = 5; $Le = L_{tow}$ = 20ft; σ_y =36,000 psi

	Buckling	Yield
S(outer)	8 in	8 in
S(inner)	7.76	7.66
Thickness, t	0.24	0.34

Table 3. Box Beam Requirements

The final consideration in the notional design of figure 45 is the design of the pins used at the pivot points of the mechanism. Shear stress is the primary concern at these points. The force acting on the pins is assumed to be the resultant of hydrodynamic resistance tension and maximum vertical force read from figure 46. $Shear\ force\ v = \sqrt{T^2 + f_{conn}^2} = 87{,}934\ pounds$. From traditional solid mechanics,

$$\tau_y = 0.5\sigma_y$$
$$v(safetyfactor) = 2\tau_y A$$

Resulting in a solid circular pin of diameter $3.94" \approx 4"$.

C. CONCLUSIONS AND RECOMENDATIONS

1. Conclusions

SLICE-KAIMALINO close proximity towing operations are feasible based on analysis of regular and random wave vertical plane vessel response. The close proximity-towing concept promises to be a cost effective means to transport a wide range of payload configurations at high speed. It may also result in the development of versatile warships capable of multiple roles as fighting ships and payload delivery platforms. The goal of this research, to provide an estimate of SWATH vessel motions and connection forces based on a generic connection has been accomplished in heave and pitch. Since heave and pitch are expected to be the most violent motions constrained between the vessels, these motions are likely to result in the highest magnitude connection forces. With this in mind, the analysis shows that connection forces are manageable with reasonably sized handling equipment. The research also reveals trends in the operating characteristics of the vessels, and insight into the optimization of spring-damper values that should be designed into the connection. In particular, head seas provided the highest magnitude forces. Three, six, and twelve knots yielded peak absolute motions and connection forces. Connection force response characteristics changed from following seas dominated at wave height less than four feet, and head seas dominated greater than four feet. A what if analysis of spring and damping constants yielded optimum values of k and c in the three to seven thousand range. Finally, a simplified solid mechanics evaluation of the vertical forces resulted in a 20 feet long box beam with side length of 8" and a thickness of 0.34", whose thickness was dictated by yield stress.

2. Recommendations

This thesis provides a solid foundation upon which future study of close proximity towing operations can be based. Data files describing SLICE and KAIMALINO operating characteristics have been developed for motion in six degrees of freedom over a large range of environmental conditions. Related software and the process to analyze random wave results and design a notional tow bar are outlined. However, several important follow on studies should be conducted to fully validate the close proximity-towing concept. First, the software should be modified to include absolute motions and connection forces in all six degrees of freedom to confirm the assumption that vertical forces will be most significant. Next, further analysis and more complete modeling of the spring and damper constants as they relate to a notional structure should be conducted. A finite element model of the connection should be constructed to fully evaluate stress states and critical locations. Finally, tow tank scale models of the notional design should be built and evaluated to confirm simulation results and determine the effects of close field interactions between the vessels.

LIST OF REFERENCES

Beck, R. F., and Troesch, A. W., "Documentation and User's Manual for the Computer Program SHIPMO.BM," Report No. 89-2, 1989.

Cummins, W. E., "Principles of Naval Architecture, Volume III, Chapter III, 1989.

Healey, A. J., "Kalman Filtering for Sensor Fusion," Naval Postgraduate School, Monterey, CA, March 2001.

Lesh, D. B., "Seakeeping Characteristics of SLICE Hulls: A Motion Study in Six Degrees of Freedom," Naval Postgraduate School, Monterey, CA, September 1995.

Lockheed Missile and Space Company, Inc. (LMSC), "SLICE Inboard Profile," Drawing No. P1-100-04, August 1994.

Lockheed Missile and Space Company, Inc. (LMSC), "SLICE Lines and Offsets," Drawing No. P1-100-01, Sheets 1 and 2, December 1994.

Lockheed Missile and Space Company, Inc. (LMSC), "SLICE Advanced Technology Demonstration, Final Technical Review," December 1995.

Lockheed Missile and Space Company, Inc. (LMSC), "KAIMALINO Lines and Offsets," GSH generated drawings, August 1994.

McCreight, K. K., "A Note on the Selection of Wave Spectra for Design Evaluation," Naval Surface Warfare Center, January 1998.

Ochi, J. K., and Hubble, E. N., "On Six-Parameter Wave Spectra," Proceeding of the Fifteenth Conference on Coastal Engineering, July 1976.

Papoulias, F. A., "Dynamics and Control of Marine Vehicles," Informal Lecture Notes for ME4823, Naval Postgraduate School, Monterey, CA, June 1993.

Pierson, W. J., "The Spectral Ocean Wave Model (SOWM), A Northern Hemisphere Computer Model for Specifying and Forecasting Ocean Wave Spectra," DTNSRDC Report 82/011, July 1982.

THIS PAGE INTENTIONALLY LEFT BLANK

APPENDIX A

Input file, SHIPMO.IN for running regular and irregular wave analyses on the SLICE hull form. Refer to Appendix A of the SHIPMO.BM User's Manual for format and line content information.

```
SLICE HULL FORM GENERATED BY D.B. LESH APRIL 1995
Updated by NASH JAN 2001
Vertical and horizontal motions with updated surge
damping
    0     0     0     0     1     0     1     0     0     0
    1     0     1    20     1
  105.0000        1.9905      32.1740                1.26E-05
  1.6557E+02     0.0000
   33.0000  -26.0000    1.0000
    1    48.6000    0.0000     0
   16.5000    0.0000
    5    44.8750    0.0000     0
   16.0000    0.0000
   16.2500   -0.9000
   16.5000   -1.8000
   16.7500   -0.9000
   17.0000    0.0000
    8    40.8750    0.0000     0
   15.5000    0.0000
   15.8000   -2.0000
   16.1000   -4.0000
   16.1000  -10.0000
   16.9000  -10.0000
   16.9000   -4.0000
   17.2000   -2.0000
   17.5000    0.0000
   15    39.8750    0.0000     0
   15.4000    0.0000
   15.6000   -1.5000
   15.5500   -7.3100
   14.6250   -8.9200
   14.5000  -10.0000
   14.6250  -11.1000
   15.0850  -11.4100
   16.5000  -12.0000
   17.9000  -11.4100
   18.3750  -11.1000
   18.5000  -10.0000
   18.3750   -8.9200
```

17.4500	-7.3100		
17.4000	-1.5000		
17.6000	0.0000		
11	37.8750	0.0000	0
15.0000	0.0000		
15.0000	-5.7500		
13.5800	-8.3125		
13.3000	-10.0000		
14.7000	-11.7900		
16.5000	-13.2000		
18.2900	-11.7900		
19.7000	-10.0000		
19.4200	-8.3125		
18.0000	-5.7500		
18.0000	0.0000		
15	33.8750	0.0000	0
14.8750	0.0000		
14.8750	-4.8000		
14.8500	-4.9100		
13.0400	-8.0000		
12.5000	-10.0000		
13.0400	-12.0000		
14.5000	-13.4600		
16.5000	-14.0000		
18.5000	-13.4600		
20.0000	-12.0000		
20.5000	-10.0000		
20.0000	-8.0000		
18.1500	-4.9100		
18.1250	-4.8000		
18.1250	0.0000		
13	23.8750	0.0000	0
15.2000	0.0000		
15.2000	-6.9200		
13.0400	-8.0000		
12.5000	-10.0000		
13.0400	-12.0000		
14.5000	-13.4600		
16.5000	-14.0000		
18.5000	-13.4600		
20.0000	-12.0000		
20.5000	-10.0000		
20.0000	-8.0000		
17.8000	-6.9200		
17.8000	0.0000		
13	19.8750	0.0000	0
15.8750	0.0000		

```
15.9100   -6.1200
15.6640   -6.5500
13.0380  -10.0000
13.5000  -11.7300
14.7700  -13.0000
16.5000  -13.4600
18.2300  -13.0000
19.5000  -11.7300
20.0000  -10.0000
17.3400   -6.5500
17.1000   -6.1200
17.1250    0.0000
15    16.8750     0.0000     0
16.4000    0.0000
16.4000   -7.2500
15.0600   -7.5100
14.0100   -8.5600
13.6200  -10.0000
14.0100  -11.4400
15.0600  -12.4900
16.5000  -12.8800
18.0000  -12.4900
19.1000  -11.4400
19.3800  -10.0000
19.1000   -8.5600
18.0000   -7.5100
16.6000   -7.2500
16.6000    0.0000
13      7.1250     0.0000     1
16.5000   -9.2800
16.1400   -9.3800
15.8800   -9.6400
15.7800  -10.0000
15.8800  -10.3600
16.1400  -10.6200
16.5000  -10.7200
16.8600  -10.6200
17.1200  -10.3600
17.2200  -10.0000
17.1200   -9.6400
16.8600   -9.3800
16.5000   -9.2800
 1     0.0000     0.0000     1
23.5000    0.0000
 1   -10.1250     0.0000     1
23.5000  -10.0000
13   -11.3000     0.0000     1
```

```
23.5000    -7.8000
22.4000    -8.0900
21.5900    -8.9000
21.3000   -10.0000
21.5900   -11.1000
22.4000   -11.9100
23.5000   -12.2000
24.6000   -11.9100
25.4000   -11.1000
25.7000   -10.0000
25.4000    -8.9000
24.6000    -8.0900
23.5000    -7.8000
13   -13.3500     0.0000     1
23.5000    -7.1000
22.1000    -7.4800
21.0800    -8.5500
20.6000   -10.0000
21.1800   -11.4500
22.1500   -12.5200
23.5000   -12.9000
25.0000   -12.5200
26.0000   -11.4500
26.4000   -10.0000
26.0000    -8.5500
25.0000    -7.4800
23.5000    -7.1000
15   -16.7900     0.0000     0
22.4000     0.0000
23.4000    -6.0000
21.5000    -6.5400
20.0000    -8.0000
19.5000   -10.0000
20.0000   -12.0000
21.5000   -13.4600
23.5000   -14.0000
25.5000   -13.4600
27.0000   -12.0000
27.5000   -10.0000
27.0000    -8.0000
25.5000    -6.5400
23.6000    -6.0000
24.6000     0.0000
11   -19.1250     0.0000     0
22.1000     0.0000
22.1000    -5.3000
21.3400    -6.6350
```

```
19.5000  -10.0000
20.6700  -12.8300
23.5000  -14.0000
26.3300  -12.8300
27.5000  -10.0000
25.6600   -6.6350
24.9000   -5.3000
24.9000    0.0000
13   -25.1250     0.0000     0
21.9000    0.0000
21.9000   -5.0000
21.7500   -5.0500
20.0000   -8.0000
19.5000  -10.0000
20.6700  -12.8300
23.5000  -14.0000
26.3300  -12.3300
27.5000  -10.0000
27.0000   -8.0000
25.2600   -5.0500
24.9000   -5.0000
24.9000    0.0000
13   -32.1250     0.0000     0
22.0000    0.0000
22.0000   -6.8000
22.0250   -6.8800
21.6700   -7.4900
20.3000  -10.0000
21.2400  -12.2600
23.5000  -14.0000
25.7000  -12.2600
26.7000  -10.0000
25.3300   -7.4900
25.0000   -6.8800
25.0000   -6.8000
25.0000    0.0000
15   -40.8000     0.0000     0
23.4000    0.0000
23.4000   -8.8000
23.0000   -8.9750
22.5000   -9.4100
22.3200  -10.0000
22.5000  -10.5900
23.0000  -11.0200
23.5000  -11.8300
24.0900  -11.0200
24.5200  -10.5900
```

```
  24.6800  -10.0000
  24.5200   -9.4100
  24.0000   -8.9750
  23.6000   -8.8000
  23.6000    0.0000
   1  -46.1250    0.0000    1
  23.5000  -10.0000
   0.1000    0.0000
   2.0400       0.0       0.0
   2962
7  -46.00    0.0000    9.5000
    1.0000    20.0000  1000.0000     20.0000     00.00
    00.0000    0.0000
    0.1000
 005.0000  005.0000    0.0000
 0.0
```

APPENDIX B

Input file, SHIPMO.IN for running regular and irregular wave analyses on the KAIMALINON hull form. Refer to Appendix A of the SHIPMO.BM User's Manual for format and line content information.

```
     KAIMALINO horizontal and vertical motions
     With surge damping
     Generated by C.A. Nash Jan 2001

          0     0     0     0     1     0     1     0     0     0
          1     0     1    20     1
       80.50000       1.9905      32.1740                  1.26E-05
2.6500E+02    0.0000
        33.0000   -26.0000    1.0000
        15    40.5000     0.0000    1
        19.6120   -11.0630
        19.2830   -11.2830
        19.1560   -11.4370
        19.0900   -12.0000
        19.1900   -12.3800
        19.3700   -12.6000
        19.7400   -13.0140
        20.1980   -12.9950
        20.5630   -12.8440
        20.8440   -12.5630
        20.9950   -12.1980
        20.9950   -11.8020
        20.8440   -11.4370
        20.5930   -11.1560
        20.1980   -11.0630
        13    38.5000     0.0000    1
        19.4100    -9.0100
        18.3100    -9.4600
        17.4700   -10.3100
        16.9700   -11.7000
        17.8500   -14.1500
        19.1200   -14.9200
        20.3000   -15.0300
        21.6900   -14.5300
        22.5400   -13.6900
        23.0340   -12.2990
        22.9200   -11.1100
        22.1600    -9.8400
```

20.8900	-9.0100		
15	34.5000	0.0000	0
18.5200	2.5340		
19.5300	-2.9700		
19.5300	-8.8000		
18.2000	-9.3100		
17.5000	-9.9300		
16.7800	-11.6800		
17.1500	-13.5200		
19.0000	-15.1600		
20.3200	-15.2190		
22.6900	-13.8000		
23.2400	-12.0000		
22.6400	-10.2000		
20.4700	-8.8000		
20.4700	-2.9700		
21.2100	2.5340		
14	28.5000	0.0000	0
18.2000	0.0000		
19.0700	-8.8600		
18.1800	-9.2700		
16.7400	-11.6800		
16.8600	-12.9500		
17.6800	-14.3200		
19.3600	-15.2170		
21.2600	-15.0300		
22.5400	-14.0800		
23.2600	-12.3200		
23.1450	-11.0500		
22.3200	-9.6800		
20.9400	-8.8600		
21.8100	0.0000		
14	26.5000	0.0000	0
18.0200	0.0000		
18.8800	-8.9000		
17.2500	-10.1600		
16.7100	-11.6800		
17.0800	-13.5600		
18.1600	-14.7500		
20.0000	-15.3100		
21.8400	-14.7500		
23.1700	-12.9600		
23.2900	-12.3200		
22.3400	-9.6600		
21.3100	-8.9700		
20.1000	-8.7000		
21.9700	0.0000		

```
14   22.5000     0.0000     0
18.2700   -0.2500
20.0000   -8.6300
18.8250   -8.8500
17.2000  -10.1300
16.6400  -11.6700
17.0300  -13.5900
18.7100  -15.1200
20.3300  -15.3560
21.5900  -14.9700
22.8000  -13.8700
23.3600  -11.6700
22.6100   -9.8600
21.2800   -8.8900
21.7000   -0.2500
14   20.5000     0.0000     0
18.4800    0.0000
19.9900   -7.6700
18.8600   -7.8000
16.2300   -9.4800
15.5000  -11.1100
16.2300  -14.5200
18.6800  -16.3400
20.4500  -16.5200
22.5200  -15.7730
23.7700  -14.5200
24.5400  -12.0000
23.7700   -9.4800
21.2200   -7.8400
21.5100   -0.0300
15   15.0000     0.0000     0
19.7700   -0.8500
20.0000   -7.2200
17.9000   -8.1500
16.0300   -9.3500
15.2500  -11.5300
15.4300  -13.3900
16.9700  -15.6900
19.0700  -16.6800
20.4700  -16.7500
22.6500  -15.9700
24.6800  -12.9300
24.6800  -11.0700
23.6900   -8.9700
20.2700   -7.2400
20.2900   -0.9500
13   6.5000     0.0000     1
```

19.5300	-7.2400		
16.9600	-8.3000		
15.4200	-10.6100		
15.2300	-12.4700		
16.3000	-15.0400		
18.1700	-16.4200		
20.4700	-16.7900		
22.6600	-15.9800		
23.9800	-14.6590		
24.7600	-12.4700		
24.5800	-10.6100		
23.0400	-8.3000		
21.3900	-7.4200		
15	2.5000	0.0000	1
19.5300	-7.2300		
17.3400	-8.0200		
16.0200	-9.3400		
15.2300	-11.5300		
15.5700	-13.8300		
17.3400	-15.9900		
19.0700	-16.7000		
20.0000	-16.7900		
20.9400	-16.7000		
22.6600	-15.9900		
24.4300	-13.8300		
24.7800	-11.5300		
23.9900	-9.3400		
22.6600	-8.0200		
20.4700	-7.2300		
15	0.0000	0.0000	1
19.5300	-7.2300		
17.3400	-8.0200		
16.0200	-9.3400		
15.2300	-11.5300		
15.5700	-13.8300		
17.3400	-15.9900		
19.0700	-16.7000		
20.0000	-16.7900		
20.9400	-16.7000		
22.6600	-15.9900		
24.4300	-13.8300		
24.7800	-11.5300		
23.9900	-9.3400		
22.6600	-8.0200		
20.4700	-7.2300		
15	-3.5000	0.0000	1
19.5300	-7.2300		

```
17.3400    -8.0200
16.0200    -9.3400
15.2300   -11.5300
15.5700   -13.8300
17.3400   -15.9900
19.0700   -16.7000
20.0000   -16.7900
20.9400   -16.7000
22.6600   -15.9900
24.4300   -13.8300
24.7800   -11.5300
23.9900    -9.3400
22.6600    -8.0200
20.4700    -7.2300
15    -7.5000     0.0000     1
19.5300    -7.2300
17.3400    -8.0200
16.0200    -9.3400
15.2300   -11.5300
15.5700   -13.8300
17.3400   -15.9900
19.0700   -16.7000
20.0000   -16.7900
20.9400   -16.7000
22.6600   -15.9900
24.4300   -13.8300
24.7800   -11.5300
23.9900    -9.3400
22.6600    -8.0200
20.4700    -7.2300
15   -11.5000     0.0000     0
19.5500    -0.1500
20.0300    -1.8500
19.5300    -7.2300
16.0200    -9.3400
15.2300   -11.5300
16.1300   -14.5500
17.3400   -15.9900
19.0700   -16.7000
20.9400   -16.7000
22.6600   -15.9900
24.4300   -13.8300
24.7800   -11.5300
23.9900    -9.3400
21.2400    -7.1500
20.3700    -0.2500
15   -15.5000     0.0000     0
```

```
18.7200   -0.5200
19.1700   -2.9700
19.1900   -7.6300
17.4800   -8.2300
15.8100  -10.2600
15.4600  -12.0000
17.1200  -15.5100
20.0000  -16.5400
22.1400  -16.0000
24.5100  -12.4400
24.1900  -10.2600
22.8800   -8.4900
20.8100   -7.6300
20.8300   -2.9700
21.2700   -0.5200
15   -19.5000     0.0000     0
18.2400   -0.7700
18.4500   -2.9700
20.0000   -8.2500
18.6200   -8.5500
16.6400  -10.2000
16.2100  -11.6300
17.3000  -14.7000
20.0000  -15.8100
22.0000  -15.3300
23.1700  -14.1200
23.8000  -11.6300
23.3600  -10.2000
21.3800   -8.5500
21.5600   -2.9700
21.7600   -0.7700
15   -23.5000     0.0000     0
18.1300   -0.9900
18.6200   -5.9700
18.1400   -5.9700
18.6200   -9.4500
17.0100  -11.7100
17.8800  -14.1200
20.0000  -15.0000
21.1500  -14.7700
22.5000  -13.6600
22.9900  -11.7100
22.3200  -10.1000
21.3800   -9.4500
21.3800   -5.9700
21.8600   -5.9700
21.8700   -0.9900
```

```
          14   -32.7500     0.0000     0
          19.1800    -0.6500
          18.7600    -2.9700
          18.7600    -5.9700
          20.0000   -11.2700
          19.4400   -11.5400
          19.2800   -12.0000
          19.5400   -12.5600
          19.8600   -12.7100
          20.4000   -12.6000
          20.7300   -12.0000
          20.4600   -11.4400
          21.2500    -5.9700
          21.2500    -2.9700
          20.8200    -0.6500
          11   -36.0000     0.0000     1
          19.8900    -2.2500
          19.6900    -5.9700
          19.5000    -6.1500
          19.6100    -9.9100
          19.8200   -13.7900
          19.9700   -14.6200
          20.1800   -13.7900
          20.4000    -9.9100
          20.5000    -6.1500
          20.3100    -5.9700
          20.0000    -1.8400
           4   -40.0000     0.0000     1
          19.9900    -6.1700
          19.9900   -15.1700
          20.0100   -15.1700
          20.0100    -6.1700
           0.2     0.0000
           2.6750        0.0        0.0
           0
       7  40.0000    0.0000    9.5000
          1.0000     20.0000   1000.0000     20.0000     13.502
13.502     0.0000
          0.1000
        170.0000  170.0000    0.0000
        0.0
```

THIS PAGE INTENTIONALLY LEFT BLANK

APPENDIX C

"MATDATA" output files generated by SHIPMO.IN. These files provide regular wave response mass added and excitation force matrix constants for given ship, speed, and wave angle. File names are described in the following format:

m -matdata.
s or k -Vessel simulated, s-SLICE; k-KAIMALINO.
v or vh -Motion simulated, v-vertical; vh-all six degrees of freedom.
Speed -Zero to twenty knots in one-knot increments.
Angle -Zero to 180 degrees in five-degree increments.

Example:
mkvh5_180.txt = Kaimalino, motion in 6-dof, at 5 knots, 180° wave angle.

SLICE matdata files	KAIMALINO matdata files
mkvh0_0.txt	msvh0_0.txt
mkvh1_0.txt	msvh1_0.txt
mkvh2_0.txt	msvh2_0.txt
mkvh3_0.txt	msvh3_0.txt
mkvh4_0.txt	msvh4_0.txt
mkvh5_0.txt	msvh5_0.txt
.	.
.	.
.	.
mkvh20_0.txt	**msvh20_0.txt**
mkvh0_5.txt	msvh0_5.txt
mkvh1_5.txt	msvh1_5.txt
mkvh2_5.txt	msvh2_5.txt
.	.
.	.
.	.
mkvh20_180.txt	**msvh20_180.txt**

(2 ships) X (21 speeds) X (37 angles) = 1554 files

THIS PAGE INTENTIONALLY LEFT BLANK

APPENDIX D

```
% samplemain.m
% This file takes input speed, heading, spring const., and damping constants
% and returns regular and random wave response in the vertical plane.
%       Shipmo output files (matdata) are loaded.
%       Coupled heave-pitch response of the Slice and Kaimalino are modeled:
%       Parametric studies conducted on input variables.
% Results are used in graphics program where significant force is plotted versus
% x-coordinates specified for different values of parametric variable.
%
% Dimensional version (U.S. units)
% Get run info
%
clear
kcount=1;
T=35000;
%Kaimalino resistance for V=15kts, (#)
Ltow=[10:2:20];
%Range of tow lengths
k_connection=T./Ltow;
%HS=[0:2:10];
%Not used in this version since
%HScount=1;
%HS is defined in loop
Vkt=15;
Vcount=1;
betacount=1;
betadeg=180;
%input('Heading (deg) = ');
ccount=1;
c_connection=0;
%input;('Damping constant (pound.sec/ft) = ');

while kcount~=(length(Ltow)+1),          %Loop of values varied for
                                         % parametric study
  HScount=1;                             %counter for x coordinate
  HS=[0:2:10];                           %X-coordinate of parametric plot
  while HScount~=(length(HS)+1);         %create Y-coord for a parametric
                                         %input and range of X-coordinates.

      K_connection=k_connection(kcount)+i*c_connection(ccount);
      V_string=num2str(Vkt(Vcount));
      beta_string=num2str(betadeg(betacount));
```

```
%The matdata output files default to the vertical only format when the
%heading angle is 0 or 180 degrees.

%Set up file reading format:
trigg = 30;
f3loc = 27; f5loc=29;
if betadeg(betacount)==0
  trigg = 27;
  f3loc = 26; f5loc=27;
elseif betadeg(betacount)==180
trigg = 27;
  f3loc = 26; f5loc=27;
end

%
% Load FRONT SHIP data file msvhV_beta.txt
%
load_filename=strcat('msvh',V_string,'_',beta_string,'.txt');
filename_s=load(load_filename);
%
% Load REAR SHIP data file
%
load_filename=strcat('mkvh',V_string,'_',beta_string,'.txt');
filename_k=load(load_filename);
%
% GENERAL DATA
%
V=Vkt*1.6878;                       % Convert to ft/sec
lambda_min=20;                      % Min wave length (ft)
lambda_max=1000;                    % Max wave length (ft)
delta_lambda=20;                    % Wave length increment (ft)
rho=1.9905;                         % Water density
zeta=1;                             % Regular wave height
L=105;                              % Reference length
g=32.2;                             % Gravitational constant
x_s=-46;                            % FRONT SHIP attachment point
x_k=+40;                            % REAR SHIP attachment point
beta=betadeg*pi/180;
lambda=lambda_min:delta_lambda:lambda_max;
                                    % Vector of wavelengths
wavenumber=2.0*pi./lambda;          % Wave number
omega=sqrt(wavenumber*g);           % Wave frequency
omegae=omega-wavenumber*V(Vcount)*cos(beta(betacount));
                                    % Frequency of encounter
period=2.0*pi./omega;
periode=2.0*pi./omegae;
```

```
omega=omega';
omegae=omegae';
filesize=size(lambda);
lambda_size=trigg*filesize(2);
%
% FRONT SHIP
%
% Set mass matrix elements
%
M33s=filename_s(3:trigg:lambda_size,3);
M35s=filename_s(3:trigg:lambda_size,5);
M53s=filename_s(5:trigg:lambda_size,3);
M55s=filename_s(5:trigg:lambda_size,5);
%
% Added mass terms
%
A33s=filename_s(9:trigg:lambda_size,3);
A35s=filename_s(9:trigg:lambda_size,5);
A53s=filename_s(11:trigg:lambda_size,3);
A55s=filename_s(11:trigg:lambda_size,5);
%
% Damping terms
%
B33s=filename_s(15:trigg:lambda_size,3);
B35s=filename_s(15:trigg:lambda_size,5);
B53s=filename_s(17:trigg:lambda_size,3);
B55s=filename_s(17:trigg:lambda_size,5);
%
% Hydrostatic terms
%
C33s=filename_s(21:trigg:lambda_size,3);
C35s=filename_s(21:trigg:lambda_size,5);
C53s=filename_s(23:trigg:lambda_size,3);
C55s=filename_s(23:trigg:lambda_size,5);
%
% Total exciting forces
%
F3s_t_amp=filename_s(f3loc:trigg:lambda_size,5);
F5s_t_amp=filename_s(f5loc:trigg:lambda_size,5);
F3s_t_pha=filename_s(f3loc:trigg:lambda_size,6);
F5s_t_pha=filename_s(f5loc:trigg:lambda_size,6);
F3s_t=F3s_t_amp.*exp(i*F3s_t_pha.*pi/180.0);
F5s_t=F5s_t_amp.*exp(i*F5s_t_pha.*pi/180.0);
%
% Froude/Krylov exciting forces
%
```

```
F3s_f_amp=filename_s(f3loc:trigg:lambda_size,1);
F5s_f_amp=filename_s(f5loc:trigg:lambda_size,1);
F3s_f_pha=filename_s(f3loc:trigg:lambda_size,2);
F5s_f_pha=filename_s(f5loc:trigg:lambda_size,2);
F3s_f=F3s_f_amp.*exp(i*F3s_f_pha.*pi/180.0);
F5s_f=F5s_f_amp.*exp(i*F5s_f_pha.*pi/180.0);
%
% Diffraction exciting forces
%
F3s_d_amp=filename_s(f3loc:trigg:lambda_size,3);
F5s_d_amp=filename_s(f5loc:trigg:lambda_size,3);
F3s_d_pha=filename_s(f3loc:trigg:lambda_size,4);
F5s_d_pha=filename_s(f5loc:trigg:lambda_size,4);
F3s_d=F3s_d_amp.*exp(i*F3s_d_pha.*pi/180.0);
F5s_d=F5s_d_amp.*exp(i*F5s_d_pha.*pi/180.0);
%
% REAR SHIP
%
% Set mass matrix elements
%
M33k=filename_k(3:trigg:lambda_size,3);
M35k=filename_k(3:trigg:lambda_size,5);
M53k=filename_k(5:trigg:lambda_size,3);
M55k=filename_k(5:trigg:lambda_size,5);
%
% Added mass terms
%
A33k=filename_k(9:trigg:lambda_size,3);
A35k=filename_k(9:trigg:lambda_size,5);
A53k=filename_k(11:trigg:lambda_size,3);
A55k=filename_k(11:trigg:lambda_size,5);
%
% Damping terms
%
B33k=filename_k(15:trigg:lambda_size,3);
B35k=filename_k(15:trigg:lambda_size,5);
B53k=filename_k(17:trigg:lambda_size,3);
B55k=filename_k(17:trigg:lambda_size,5);
%
% Hydrostatic terms
%
C33k=filename_k(21:trigg:lambda_size,3);
C35k=filename_k(21:trigg:lambda_size,5);
C53k=filename_k(23:trigg:lambda_size,3);
C55k=filename_k(23:trigg:lambda_size,5);
%
```

```
% Total exciting forces
%
F3k_t_amp=filename_k(f3loc:trigg:lambda_size,5);
F5k_t_amp=filename_k(f5loc:trigg:lambda_size,5);
F3k_t_pha=filename_k(f3loc:trigg:lambda_size,6);
F5k_t_pha=filename_k(f5loc:trigg:lambda_size,6);
F3k_t=F3k_t_amp.*exp(i*F3k_t_pha.*pi/180.0);
F5k_t=F5k_t_amp.*exp(i*F5k_t_pha.*pi/180.0);
%
% Froude/Krylov exciting forces
%
F3k_f_amp=filename_k(f3loc:trigg:lambda_size,1);
F5k_f_amp=filename_k(f5loc:trigg:lambda_size,1);
F3k_f_pha=filename_k(f3loc:trigg:lambda_size,2);
F5k_f_pha=filename_k(f5loc:trigg:lambda_size,2);
F3k_f=F3k_f_amp.*exp(i*F3k_f_pha.*pi/180.0);
F5k_f=F5k_f_amp.*exp(i*F5k_f_pha.*pi/180.0);
%
% Diffraction exciting forces
        %
F3k_d_amp=filename_k(f3loc:trigg:lambda_size,3);
F5k_d_amp=filename_k(f5loc:trigg:lambda_size,3);
F3k_d_pha=filename_k(f3loc:trigg:lambda_size,4);
F5k_d_pha=filename_k(f5loc:trigg:lambda_size,4);
F3k_d=F3k_d_amp.*exp(i*F3k_d_pha.*pi/180.0);
F5k_d=F5k_d_amp.*exp(i*F5k_d_pha.*pi/180.0);
%
% MATCHING CONDITION
%
A33bar_s=-(omegae.^2).*(M33s+A33s)+i*omegae.*B33s+C33s;
A35bar_s=-(omegae.^2).*(M35s+A35s)+i*omegae.*B35s+C35s;
A53bar_s=-(omegae.^2).*(M53s+A53s)+i*omegae.*B53s+C53s;
A55bar_s=-(omegae.^2).*(M55s+A55s)+i*omegae.*B55s+C55s;
A33bar_k=-(omegae.^2).*(M33k+A33k)+i*omegae.*B33k+C33k;
A35bar_k=-(omegae.^2).*(M35k+A35k)+i*omegae.*B35k+C35k;
A53bar_k=-(omegae.^2).*(M53k+A53k)+i*omegae.*B53k+C53k;
A55bar_k=-(omegae.^2).*(M55k+A55k)+i*omegae.*B55k+C55k;
%
mu3_s=(A55bar_s.*F3s_t-A35bar_s.*F5s_t)./(A33bar_s.*A55bar_s-
A35bar_s.*A53bar_s);
nu3_s=(A55bar_s+A35bar_s*x_s)./(A33bar_s.*A55bar_s-
A35bar_s.*A53bar_s);
mu5_s=(A53bar_s.*F3s_t-A33bar_s.*F5s_t)./(A53bar_s.*A35bar_s-
A33bar_s.*A55bar_s);
nu5_s=(A53bar_s+A33bar_s*x_s)./(A53bar_s.*A35bar_s-
A33bar_s.*A55bar_s);
```

```
mu3_k=(A55bar_k.*F3k_t-A35bar_k.*F5k_t)./(A33bar_k.*A55bar_k-
A35bar_k.*A53bar_k);
nu3_k=(A55bar_k+A35bar_k*x_k)./(A33bar_k.*A55bar_k-
A35bar_k.*A53bar_k);
mu5_k=(A53bar_k.*F3k_t-A33bar_k.*F5k_t)./(A53bar_k.*A35bar_k-
A33bar_k.*A55bar_k);
nu5_k=(A53bar_k+A33bar_k*x_k)./(A53bar_k.*A35bar_k-
A33bar_k.*A55bar_k);
%
a=mu3_s-mu5_s*x_s-mu3_k+mu5_k*x_k;
b=nu3_s-nu5_s*x_s+nu3_k-nu5_k*x_k;
f=(K_connection*a)./(1+b.*K_connection);
%
f_s=-f;                     % Connection force on FRONT SHIP
f_k=f;                      % Connection force on REAR SHIP
eta3_s=mu3_s+nu3_s.*f_s;    % FRONT SHIP heave
eta5_s=mu5_s+nu5_s.*f_s;    % FRONT SHIP pitch
eta3_k=mu3_k+nu3_k.*f_k;    % REAR SHIP heave
eta5_k=mu5_k+nu5_k.*f_k;    % REAR SHIP pitch
xi_s=eta3_s-eta5_s*x_s;     % FRONT SHIP motion at connection
xi_k=eta3_k-eta5_k*x_k;     % REAR SHIP motion at connection
xi0_s=mu3_s-mu5_s*x_s;      % FRONT SHIP motion at connection for
                            % zero f
xi0_k=mu3_k-mu5_k*x_k;      % REAR SHIP motion at connection for
                            % zero f
%
% Random wave calculations
% Pierson-Moscowitz spectrum
%
  waveheight(HScount)=HS(HScount);
       POWER =-.032*(g/HS(HScount))^2;
       S    =(0.0081*g^2).*exp(POWER./(omega.^4))./(omega.^5);
       % Convert S(w) to S(we)
       Se   =S./(1-(2.0/g)*omega*V(Vcount)*cos(beta(betacount)));
                  %
       % Define response spectra
       %
       Sf     =((abs(f)).^2).*Se;
       Sxi_s  =((abs(xi_s)).^2).*Se;
       Sxi_k  =((abs(xi_k)).^2).*Se;
       Sxi0_s =((abs(xi0_s)).^2).*Se;
       Sxi0_k =((abs(xi0_k)).^2).*Se;
       SF3s_t =((abs(F3s_t)).^2).*Se;
       SF3k_t =((abs(F3k_t)).^2).*Se;
       %
       % Initializations
```

```
        %
        Sf_i=0;
        Sxi_s_i=0;
        Sxi_k_i=0;
        Sxi0_s_i=0;
        Sxi0_k_i=0;
        SF3s_t_i=0;
        SF3k_t_i=0;
        %
        % Integral S(w)*|RAO|^2
        %
    for I=2:1:filesize(2),
        Sf_i     = Sf_i     + 0.5*(Sf(I)     + Sf(I-1))     * (omegae(I-1)-
        omegae(I));
         Sxi_s_i = Sxi_s_i  + 0.5*(Sxi_s(I)  + Sxi_s(I-1))  * (omegae(I-1)-
        omegae(I));
         Sxi_k_i = Sxi_k_i  + 0.5*(Sxi_k(I)  + Sxi_k(I-1))  * (omegae(I-1)-
        omegae(I));
        Sxi0_s_i= Sxi0_s_i + 0.5*(Sxi0_s(I) + Sxi0_s(I-1)) * (omegae(I-
        1)-omegae(I));
        Sxi0_k_i= Sxi0_k_i + 0.5*(Sxi0_k(I) + Sxi0_k(I-1)) * (omegae(I-
        1)-omegae(I));
        SF3s_t_i= SF3s_t_i + 0.5*(SF3s_t(I) + SF3s_t(I-1)) * (omegae(I-
        1)-omegae(I));
        SF3k_t_i= SF3k_t_i + 0.5*(SF3k_t(I) + SF3k_t(I-1)) * (omegae(I-
        1)-omegae(I));
    end
        %
        % Significant double amplitudes
        %
        sig_f    = 4.0*sqrt(Sf_i);
        sig_xi_s  = 4.0*sqrt(Sxi_s_i);
        sig_xi_k  = 4.0*sqrt(Sxi_k_i);
        sig_xi0_s = 4.0*sqrt(Sxi0_s_i);
        sig_xi0_k = 4.0*sqrt(Sxi0_k_i);
        sig_F3s_t = 4.0*sqrt(SF3s_t_i);
        sig_F3k_t = 4.0*sqrt(SF3k_t_i);

    sig_fk(HScount,kcount)=sig_f;       %(xcoord-row, param. var-col)
    HScount=HScount+1;                  % X-coord. counter
end
kcount=kcount+1;                        %Parametric variable counter
end
%
%call graphics program:
samplegraphpm
%samplegraphpm.m
```

```
%This program is for output graphics from samplemain.m
%Parametric plots of significant force vs. x-variable plotted
%for varied parametric values.
format bank
figure(1)                                    %Sig. force Amplitudes vs HS for
                                             %varied k's  (T/Ltow)

kstrng=num2str(k_connection);
%wavestr=num2str(waveheight);
cstrng=num2str(c_connection);
plot(HS,sig_fk)
grid
titlstr=['  Sig. force vs. H_{1/3} for \beta= ',beta_string,'^o',' V= ',V_string,'kts ',' c=',cstrng];
title([titlstr])
xlabel('H_{1/3}')
ylabel('\sigma_f')
```

```
%maingraph.m
%This program is for output graphics from samplemain.m
%
figure(1)
%absolute motion magnitude vs omega
kstrng=num2str(k_connection);
cstrng=num2str(c_connection);
plot(omega,abs(xi_s),'S',omega,abs(xi_k),'o',omega,abs(xi_s),omega,abs(xi_k))
grid
titlstr=['Absolute motion magnitude vs frequency (rad/sec) for k= ',kstrng,' c=',
cstrng];
title([titlstr])
xlabel('omega')
ylabel('MAGNITUDE(xi_s,xi_k)')
string1='xi_s'; string2='xi_k';
legend(string1,string2)
%
%
figure(2)
%absolute motion phase angle vs omega
plot(omega,57.32*angle(xi_s),'S',omega,57.32*angle(xi_k),'o',omega,57.32*angle
(xi_s),omega,57.32*angle(xi_k))
grid
titlstr2=['Absolute motion phase angle vs frequency (rad/sec) for k= ',kstrng,' c=',
cstrng];
title([titlstr2])
xlabel('omega')
ylabel('PHASE ANGLE(xi_s,xi_k)')
legend(string1,string2)
%
%
figure(3)
%Connection force magnitude vs omega
plot(omega,abs(f_s),'S',omega,abs(f_s))
grid
titlstr=['        Connection force magnitude vs frequency (rad/sec) for k=',kstrng,'
c=', cstrng];
title([titlstr])
xlabel('omega')
ylabel('Connection force magnitude')
string1='f_s';
legend(string1)
%
%
```

```
figure(4)
%Connection force phase angle vs omega
plot(omega,57.32*angle(f_s),'S',omega,57.32*angle(f_s))
grid
titlstr=['Connection force phase angle vs frequency (rad/sec) for k=',kstrng,' c=',
cstrng];
title([titlstr])
xlabel('omega')
ylabel('Connection force phase angle')
string1='f_s';
legend(string1)
```

INITIAL DISTRIBUTION LIST

1. Defense Technical Information Center 2
   8725 John J. Kingman Road, Suite 0944
   Ft. Belvoir, VA 22060-6218

2. Dudley Knox Library 2
   Naval Postgraduate School
   411 Dyer Road
   Monterey, CA 93943-5101

3. Chairman, Code ME.. 1
   Department of Mechanical Engineering
   Naval Postgraduate School
   Monterey, CA 93943-5101

4. Professor Fotis A. Papoulias, Code ME/PA.. 3
   Department of Mechanical Engineering
   Naval Postgraduate School
   Monterey, CA 93943-5101

5. Naval Engineering Curricular Office, Code 34.. 1
   Naval Postgraduate School
   Monterey, CA 93943-5101

6. LT Christopher A. Nash 4
   21 Wainwright Dr.
   Annapolis, MD 21401